Geoid Determination by FFT Techniques

Michael G. Sideris
sideris@ucalgary.ca

Department of Geomatics Engineering
University of Calgary

Contents

- Introduction: Geoid determination by the remove-restore technique
- The Fourier transform and its properties
- Geoid undulations by **FFT**
- Optimal spectral geoid determination
- Other applications of **FFT**
- Concluding remarks

Addendum

Matching the gravimetric geoid to the GPS-levelling undulations

Georgia Fotopoulos (gfotopou@ucalgary.ca)
Dept. of Geomatics Engineering, University of Calgary

Introduction: Geoid Determination by the Remove-Restore Technique

Stokes's Boundary Value Problem

Problem definition

$$\nabla^2 T = \frac{\partial^2 T}{\partial x^2} + \frac{\partial^2 T}{\partial y^2} + \frac{\partial^2 T}{\partial z^2} = 0$$

$$\frac{\partial T}{\partial r} + \frac{2}{r} T + \Delta g = 0$$

Solution

$$T = \frac{R}{4\pi} \iint_{\sigma} \Delta g S(\psi) d\sigma \quad \Rightarrow \quad N = \frac{T}{\gamma}$$

Gravity anomalies given on the geoid
(no masses outside the boundary surface)
Terrain reductions

Terrain Reductions

(example: Helmert's Condensation)

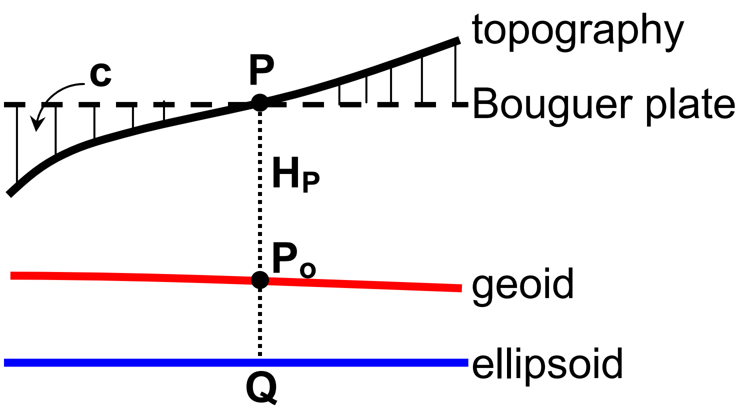

$$\Delta g_P = g_P - \gamma_Q$$

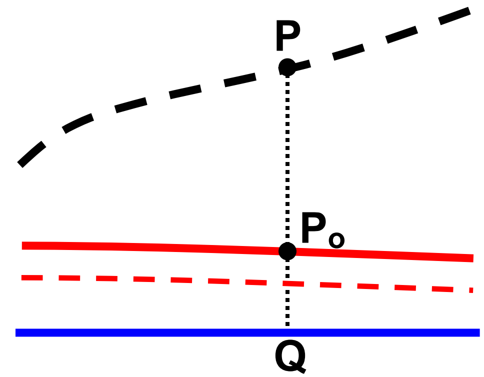

$$\Delta g'_P = \Delta g_P - A_P = \Delta g_P - BC + c$$

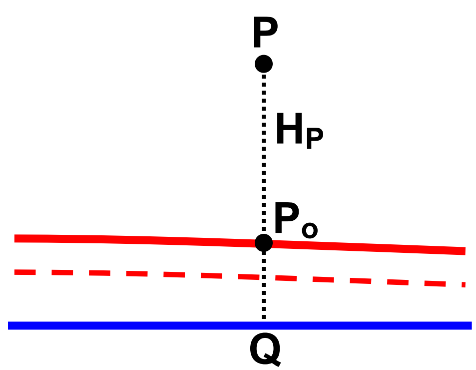

$$\Delta g'_{P_o} = \Delta g'_P + F$$

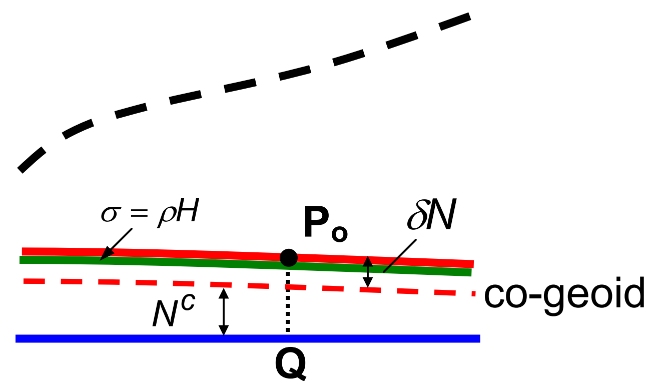

$$\Delta g_{P_o} = \Delta g'_P + F + A^c_{P_o} = \Delta g_P + F + c$$

$$= \Delta g_P^{FA} + c = \Delta g_{Faye}$$

The Remove-Restore Technique

Separate the different frequency contributions
- GM (long wavelengths)
- local gravity data (medium wavelengths)
- DTM (short wavelengths)

$$\Delta g = \Delta g^{FA} - \Delta g^{GM} - \Delta g^{H}$$

$$N = N^{GM} + N^{\Delta g} + N^{H}$$

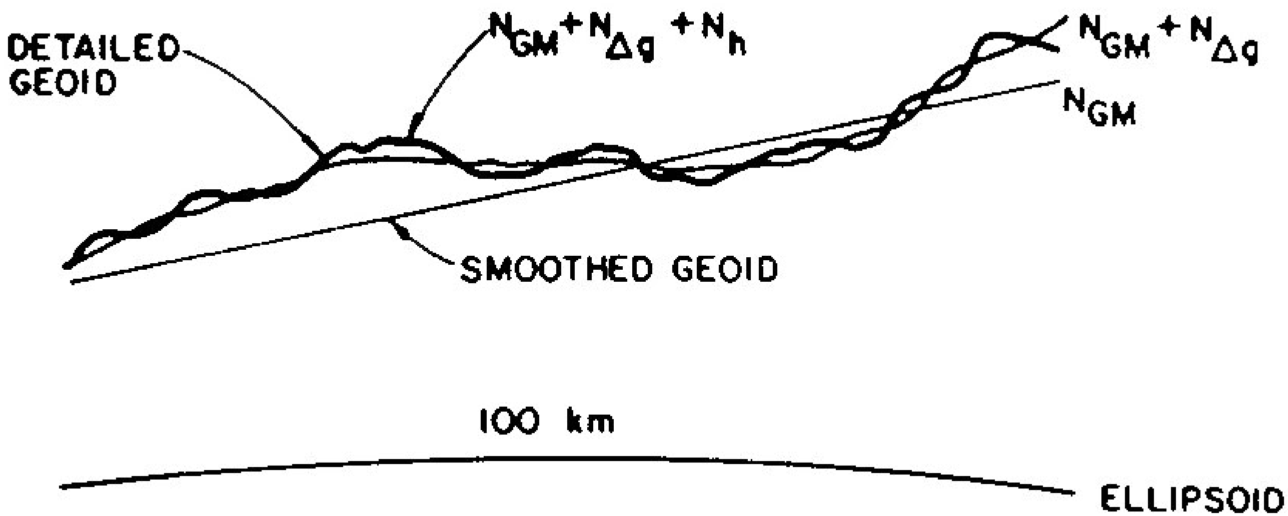

Basic Equations

GM-contributions, in spherical approximation

$$\Delta g_P^{GM} = G\sum_{n=2}^{n_{\max}}(n-1)\sum_{m=0}^{n}[C_{nm}\cos m\lambda_P + S_{nm}\sin m\lambda_P]P_{nm}(\sin\varphi_P)$$

$$N_P^{GM} = R\sum_{n=2}^{n_{\max}}\sum_{m=0}^{n}[C_{nm}\cos m\lambda_P + S_{nm}\sin m\lambda_P]P_{nm}(\sin\varphi_P)$$

Δg-contributions, in planar approximation

$$N_P^{\Delta g} = \frac{1}{2\pi\gamma}\iint_E \frac{\Delta g}{l}dxdy, \qquad l = [(x-x_P)^2 + (y-y_P)^2]^{1/2}$$

H-contributions, in planar approximation

$$\delta A_P = c_P = -\Delta g_P^H \approx \frac{1}{2}k\rho\iint_E \frac{(H-H_P)^2}{l^3}dxdy$$

$$\delta N_P \approx -\frac{\pi k\rho}{\gamma}H_P^2 - \frac{k\rho}{6\gamma}\iint_E \frac{H^3 - H_P^3}{l^3}dxdy$$

Why Use FFT?

- FFT provides very fast evaluation of convolution sums/integrals with gridded data
- In planar approximation, the Stokes and terrain correction integrals are convolutions
- In spherical approximation, these integrals are convolutions along the parallels, and so are the summations for the GM-contributions
- Gravity and topography data are usually provided on regular grids
- Computations for very large areas can be performed on a PC

The Fourier Transform and its Properties

Real Sinusoids

$s(t) = A_0 \cos(\omega_0 t + \phi_0)$:

Sinusoid of frequency ω_0

A_0 ..... *amplitude*

ω_0 ..... *cyclic frequency*

t ..... *time (or distance)*

ϕ_0 ..... *phase angle*

Expansion →

$s(t) = a \cos \omega_0 t + b \sin \omega_0 t$

where

$a = A_0 \cos \phi_0, \qquad b = -A_0 \sin \phi_0$

$A_0 = (a^2 + b^2)^{1/2}$

$\phi_0 = \arctan(\frac{-b}{a})$

$$\omega_0 = \frac{2\pi}{T_0} = 2\pi f_0$$

T_0 ..... *period*

f_0 ..... *frequency*

Sinusoids in complex form

$s_c(t) = a \cos \omega_0 t \pm i a \sin \omega_0 t = a e^{\pm i \omega_0 t}$

Real sinusoids in complex form

$s(t) = A_0 \cos(\omega_0 t + \phi_0) =$

$$A_0 \frac{e^{i(\omega_0 t + \phi_0)} + e^{-i(\omega_0 t + \phi_0)}}{2} = \frac{A_0}{2} e^{i\phi_0} e^{i\omega_0 t} + \frac{A_0}{2} e^{-i\phi_0} e^{-i\omega_0 t}$$

Fourier Series

If $g(t) = g(t+T)$; $\int_0^T g(t)dt = \int_{t_0}^{t_0+T} g(t)dt$, then

$$g(t) = \sum_{u=0}^{\infty}(a_n \cos\frac{2\pi n}{T}t + b_n \sin\frac{2\pi n}{T}t)$$

$$a_n = \frac{2}{T}\int_{t_0}^{t_0+T} g(t)\cos nt\, dt\,; \qquad b_n = \frac{2}{T}\int_{t_0}^{t_0+T} g(t)\sin nt\, dt$$

Provided that: g(t) has a finite numbers of maxima and minima in a period and a finite number of finite discontinuities (Dirichlet's conditions)

Complex form

$$g(t) = \frac{1}{T}\sum_{n=-\infty}^{\infty} G_n e^{i\omega_n t}, \qquad \omega_n = \frac{2\pi n}{T}$$

$$G_n = \int_{-T/2}^{T/2} g(t)e^{-i\omega_n t}dt, \qquad G_n = \frac{1}{2}(a_n - ib_n), \qquad n = 0, \pm 1, \pm 2, \ldots.$$

$$\text{Call } \Delta\omega = \frac{2\pi}{T} \quad \Rightarrow \quad \begin{cases} \omega_n = n\Delta\omega \\ \frac{1}{T} = \frac{\Delta\omega}{2\pi} \end{cases} \quad \Rightarrow \quad g(t) = \sum_{n=-\infty}^{\infty} \frac{G_n}{2\pi} e^{i\omega_n t}\Delta\omega$$

The Continuous Fourier Transform

$$g(t) = \frac{1}{2\pi} \int_{-\infty}^{\infty} G(\omega) e^{i\omega t} d\omega \quad \Rightarrow \quad Inverse\ CFT$$

$$G(\omega) = \int_{-\infty}^{\infty} g(t) e^{-i\omega t} dt \quad \Rightarrow \quad Direct\ CFT$$

Since $\omega = 2\pi f$ ⇒

$$g(t) = \int_{-\infty}^{\infty} G(f) e^{i2\pi ft} df \quad = \quad \boldsymbol{F}^{-1}\{G(f)\}$$

$$G(f) = \int_{-\infty}^{\infty} g(t) e^{-i2\pi ft} dt \quad = \quad \boldsymbol{F}\{g(t)\}$$

$G(f)$ is complex ⇒

$$G(f) = G_R(f) + iG_I(f) = |G(f)| e^{i\theta(f)}$$

Amplitude $\Rightarrow \quad |G(f)| = \left[G_R{}^2(f) + G_I{}^2(f)\right]^{1/2}$

Phase angle $\Rightarrow \quad \theta(f) = Arg\{G(f)\} = \arctan \dfrac{G_I(f)}{G_R(f)}$

The CTF (continued)

<u>Conditions for Existence :</u>

– The integral of $|g(t)|$ from $-\infty$ to $+\infty$ exists (it is $< \infty$)

– $g(t)$ has only finite discontinuities

– If $g(t)$ is periodic or impulse, $G(f)$ does not exist

The Impulse Function

Definition:

$$\left.\begin{aligned}&\delta(t-t_0)=0,\quad t\neq t_0\\&\int_{-\infty}^{\infty}\delta(t-t_0)\,dt=1\end{aligned}\right\}\Leftrightarrow\ \delta(t)=\lim_{a\to 0}f(t,a)$$

Definition as a distribution

$$\int_{-\infty}^{\infty}\delta(t-t_0)\phi(t)\,dt=\phi(t_0)$$

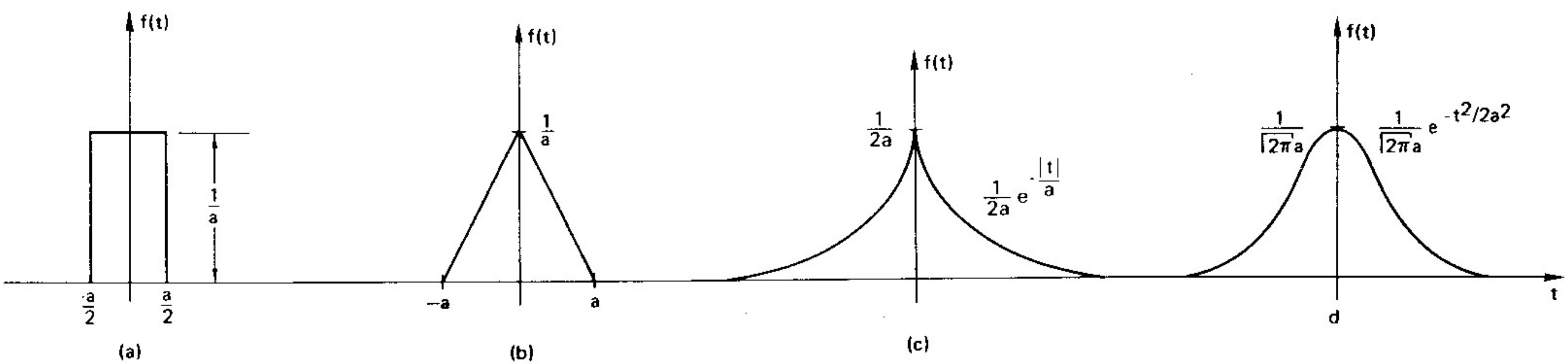

The Impulse Function (continued)

Definition as a generlized limit :

If $\lim_{n\to\infty} \int_{-\infty}^{\infty} f_n(t)\phi(t)dt = \phi(0) \quad \Rightarrow \quad \delta(t) = \lim_{n\to\infty} f_n(t)$

Properties :

$\delta(t_0)h(t) = h(t_0)\delta(t_0)$

$\delta(at) = |a|^{-1}\delta(t)$

$\boldsymbol{F}\{K\delta(t)\} = K$

e.g. If we define it as $\delta(t) = \lim_{a\to\infty} \frac{\sin at}{\pi t}$,

then $\int_{-\infty}^{\infty} \cos(2\pi ft)\, df = \int_{-\infty}^{\infty} e^{i2\pi ft}\, df = \delta(t)$

Used, as a distribution, for the (otherwise nonexistent) CFT of periodic functions

The CTF of cosine and sine

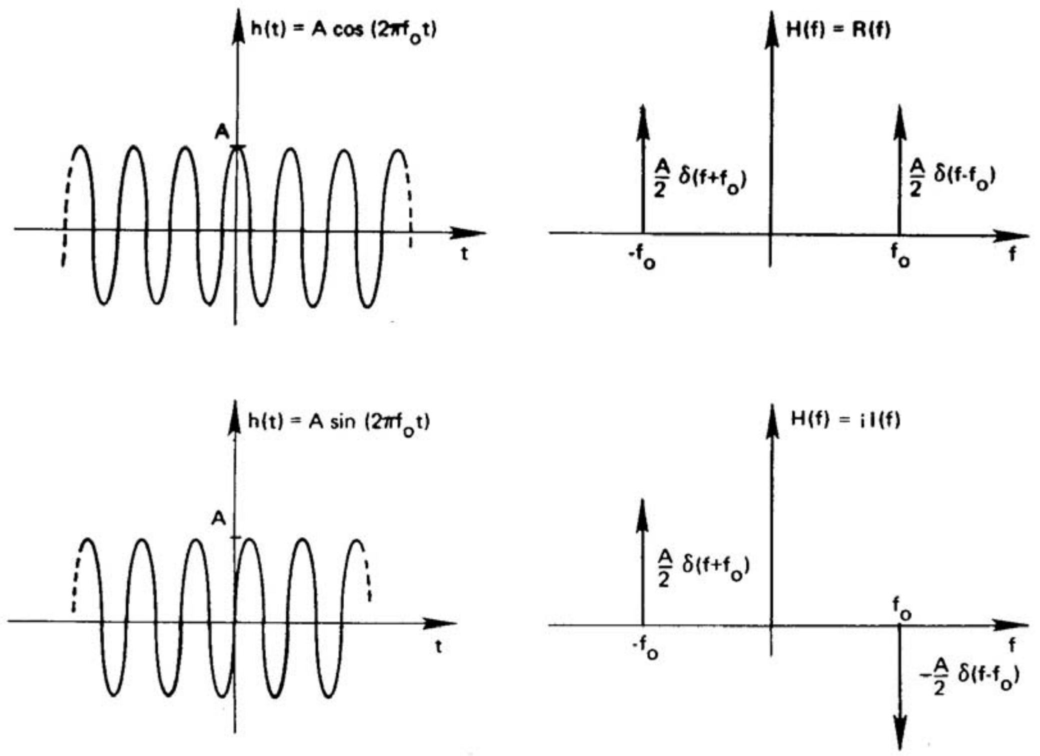

$$A\cos(2\pi f_o t) \leftrightarrow \frac{A}{2}\delta(f - f_o) + \frac{A}{2}\delta(f + f_o)$$

$$A\sin(2\pi f_o t) \leftrightarrow i\frac{A}{2}\delta(f + f_o) - i\frac{A}{2}\delta(f - f_o)$$

The Sampling Function

$$III(t) = \sum_{n=-\infty}^{\infty} \delta(t - nT) \quad \leftrightarrow \quad \boldsymbol{F}\{III(t)\} = \frac{1}{T} \sum_{n=-\infty}^{\infty} \delta(f - \frac{n}{T})$$

$$III(t)f(t) = \sum_{n=-\infty}^{\infty} f(nT)\delta(t - nT) \Rightarrow \textbf{Digitization}$$

The Rectangle and sinc Functions

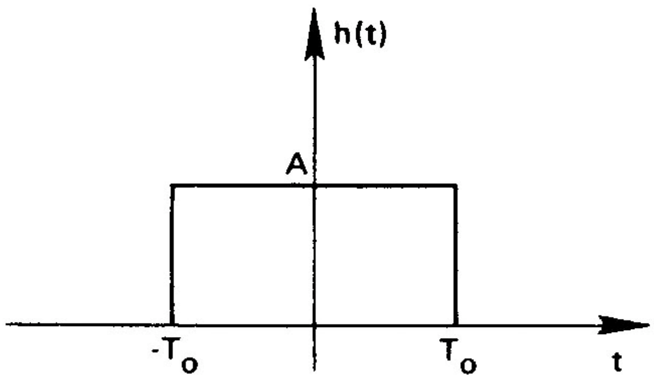

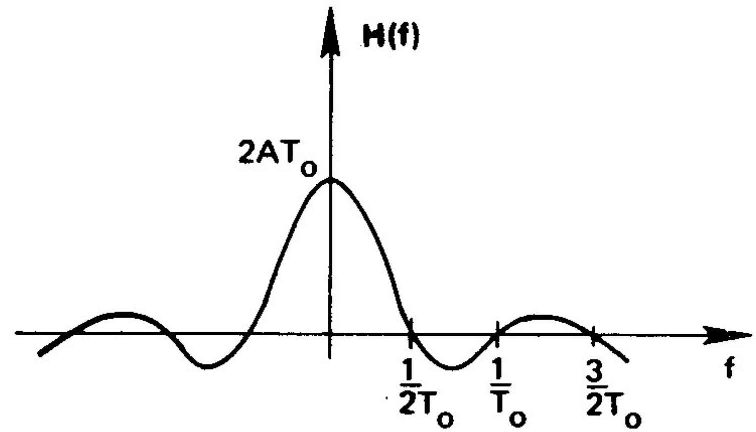

$$h(\mathrm{t}) = \begin{cases} A, & |t| = T_0/2 \\ A/2, & t = \pm T_0/2 \\ 0, & |t| > T_0/2 \end{cases} \quad \leftrightarrow \quad H(f) = 2\mathrm{AT_o}\mathrm{sinc}(2T_o f),$$

$$\mathrm{sinc}(f) = \frac{\sin(\pi f)}{\pi f}$$

Properties of the CFT

- Linearity $$ah(t) + bg(t) \leftrightarrow aH(f) + bG(f)$$
- Symmetry $$H(t) \leftrightarrow h(-f)$$
- Time scaling $$h(at) \leftrightarrow \frac{1}{|a|} H(\frac{f}{a})$$
- Time shifting $$h(t - t_o) \leftrightarrow H(f)e^{-i 2\pi f t_o}$$
- Differentiation $$\frac{\partial^n h(t)}{\partial t^n} \leftrightarrow (i 2\pi f)^n H(f)$$
- Integration $$\int_{-\infty}^{t} h(x)dx \leftrightarrow \frac{1}{i 2\pi f} H(f) + \frac{1}{2} H(0)\delta(f)$$

Properties of the CFT (continued)

- DC-value $$\int_{-\infty}^{\infty} h(t)dt = H(0)$$
- Even function $$h_E(t) \leftrightarrow H_E(f) = R_E(f)$$
- Odd function $$h_O(t) \leftrightarrow H_O(f) = iI_O(f)$$
- Real function $$h(t) = h_R(t) \leftrightarrow H(f) = R_E(f) + iI_O(f)$$
- Imaginary function $$h(t) = ih_I(t) \leftrightarrow H(f) = R_O(f) + iI_E(f)$$

Convolution and Correlation

$$x(t)=\int_{-\infty}^{\infty} g(t')h(t-t')dt' = g(t)*h(t) = h(t)*g(t) = \int_{-\infty}^{\infty} h(t')g(t-t')dt'$$

$$y(t)=\int_{-\infty}^{\infty} g(t')h(t+t')dt' = g(t)\otimes h(t) \neq h(t)\otimes g(t)$$

Convolution theorem

$$X(f)=\boldsymbol{F}\{g(t)*h(t)\}=\boldsymbol{F}\{g(t)\}\boldsymbol{F}\{h(t)\}=G(f)H(f)$$

Correlation theorem

$$Y(f)=\boldsymbol{F}\{g(t)\otimes h(t)\}=G(f)H^{*}(f)$$

Pictorial Representation of Convolution and Correlation

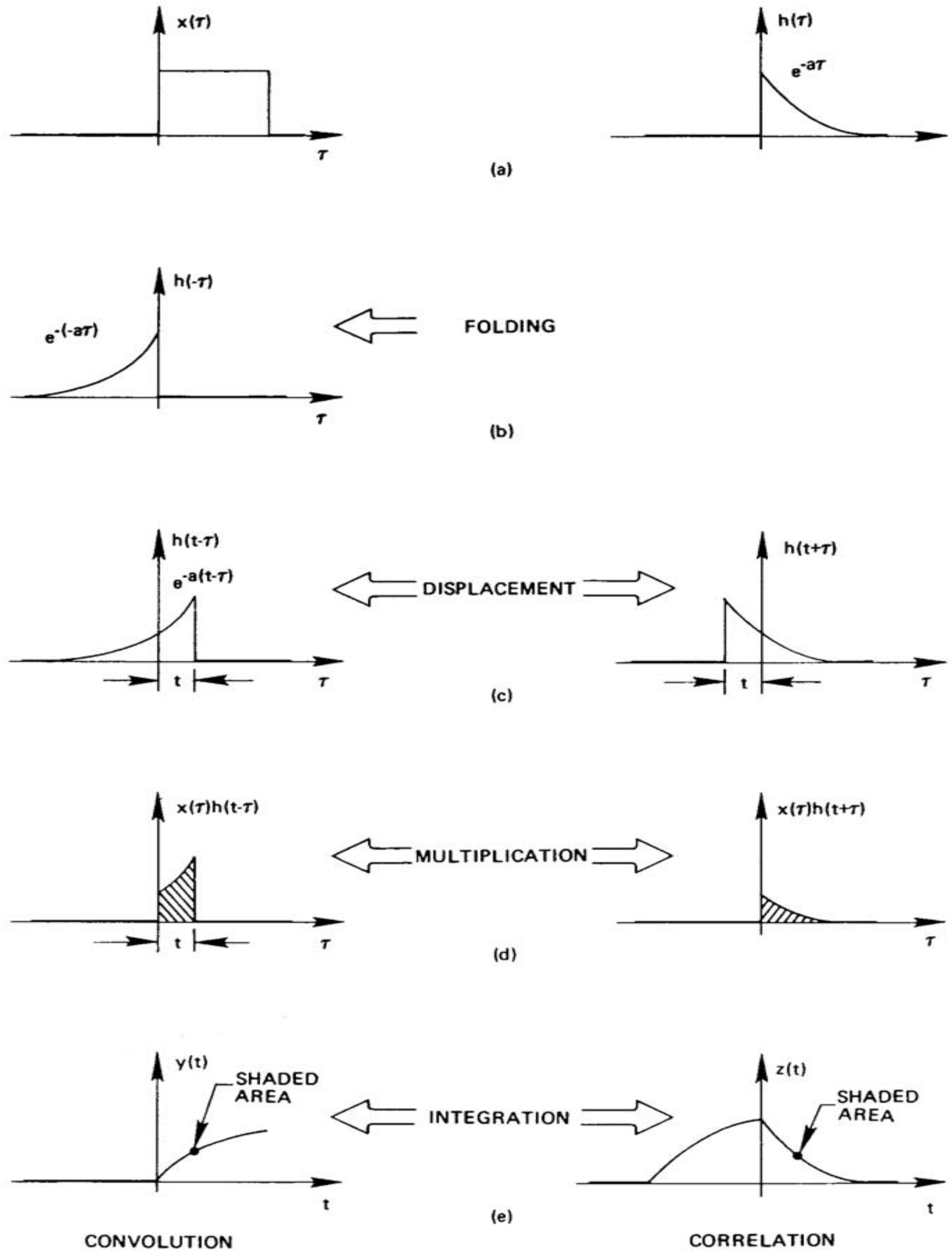

Convolution and Correlation (continued)

Properties:

a) If either $g(t)$ or $h(t)$ is even, then $g(t) * h(t) = g(t) \otimes h(t)$

b) $\delta(t+\tau) * h(t) = h(t+\tau), \qquad \delta(t) * h(t) = h(t)$

c) $x'(t) = (g(t) * h(t))' = g'(t) * h(t) = g(t) * h'(t)$

d) $\boldsymbol{F}\{h(t)g(t)\} = \boldsymbol{F}\{h(t)\} * \boldsymbol{F}\{g(t)\} = H(f) * G(f)$

e) If $h(t)$ and $g(t)$ are time limited functions, i.e, non-zero in the domain $-T_0 \le t \le T_0$, then $x(t) = h(x) * g(t)$ is time limited with twice the support of $h(t)$ or $g(t)$, i.e., non-zero in the domain $-2T_0 \le t \le 2T_0$

f) Parseval's thereom:

$$\int_{-\infty}^{\infty} h^2(t) e^{-2\pi\sigma t} dt = \int_{-\infty}^{\infty} H(f) H(\sigma - f) df$$

with $\sigma = 0$ and for $h(t)$ real: $\int_{-\infty}^{\infty} h^2(t) dt = \int_{-\infty}^{\infty} |H(f)|^2 df$

From the **Continuous** to the **Discrete** Fourier Transform

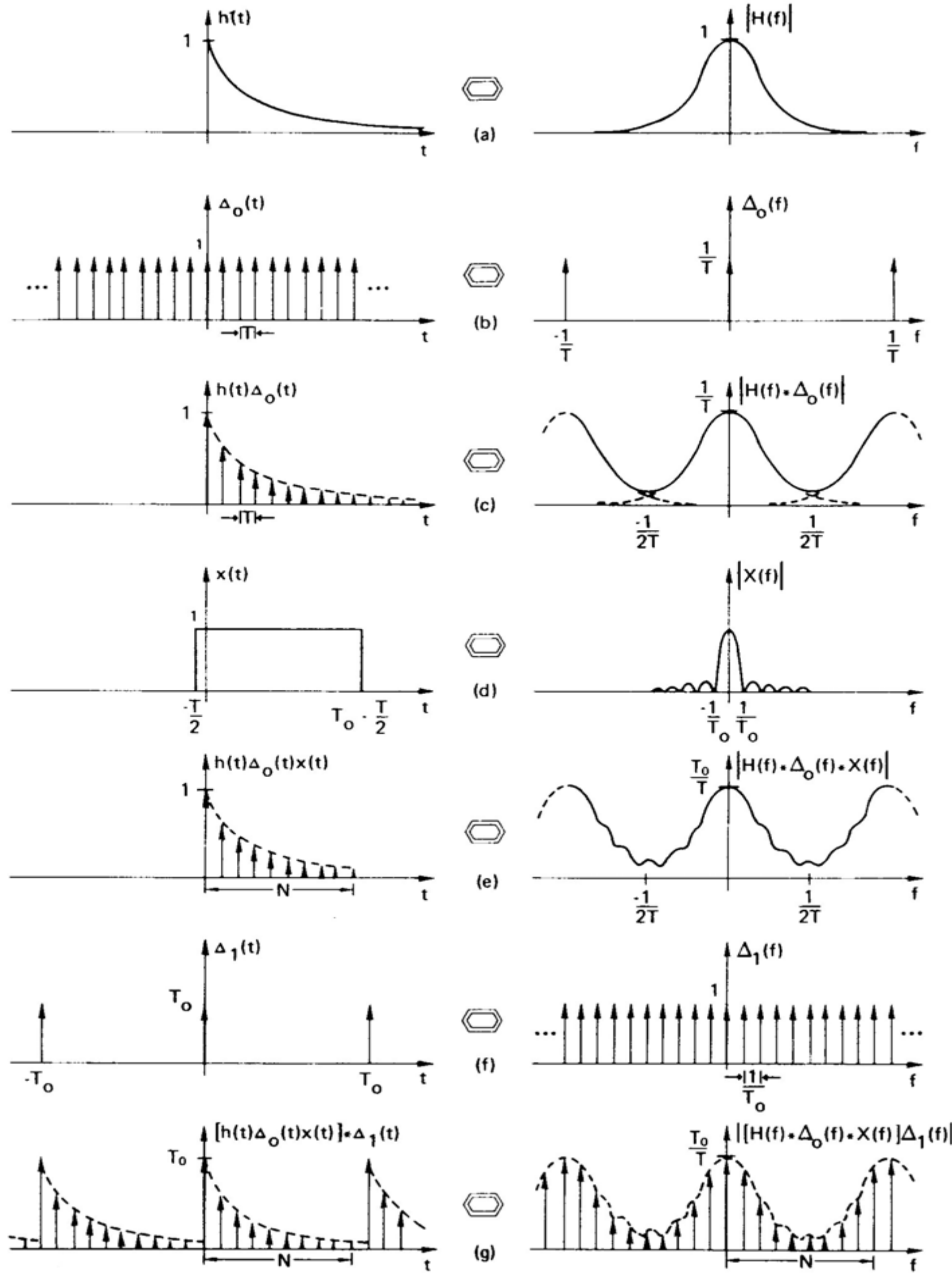

aliasing

leakage

periodic

The Discrete Fourier Transform

$$H(m\Delta f)=\sum_{k=0}^{N-1}h(k\Delta t)e^{-i2\pi k\Delta t m\Delta f}\Delta t=\sum_{k=0}^{N-1}h(k\Delta t)e^{-i2\pi km/N}\Delta t$$

$$h(k\Delta t)=\sum_{m=0}^{N-1}H(m\Delta f)e^{i2\pi k\Delta t m\Delta f}\Delta f=\sum_{m=0}^{N-1}H(m\Delta f)e^{i2\pi km/N}\Delta f$$

$$T_o=\frac{1}{\Delta f}=N\Delta t,\qquad F_o=\frac{1}{\Delta t}=N\Delta f,\qquad |f_N|=\frac{F_o}{2}=\frac{1}{2\Delta t}$$

$$h(k\Delta t)\leftrightarrow H(m\Delta f)\quad \text{or}\quad h(t_k)\leftrightarrow H(f_m)\quad \text{or}\quad h(k)\leftrightarrow H(m)$$

Discrete and circular convolution and correlation

$$x(k)=\sum_{l=0}^{N-1}g(l)h(k-l)\Delta t=g(k)*h(k)\qquad y(k)=\sum_{l=0}^{N-1}g(l)h(k+l)\Delta t=g(k)\otimes h(k)$$

$$x(k)=\boldsymbol{F}^{-1}\{\boldsymbol{F}\{g(k)\}\boldsymbol{F}\{h(k)\}\}\qquad y(k)=\boldsymbol{F}^{-1}\{\boldsymbol{F}\{g(k)\}[\boldsymbol{F}\{h(k)\}]^*\}$$

Circular Convolution as Linear Convolution Plus Aliasing

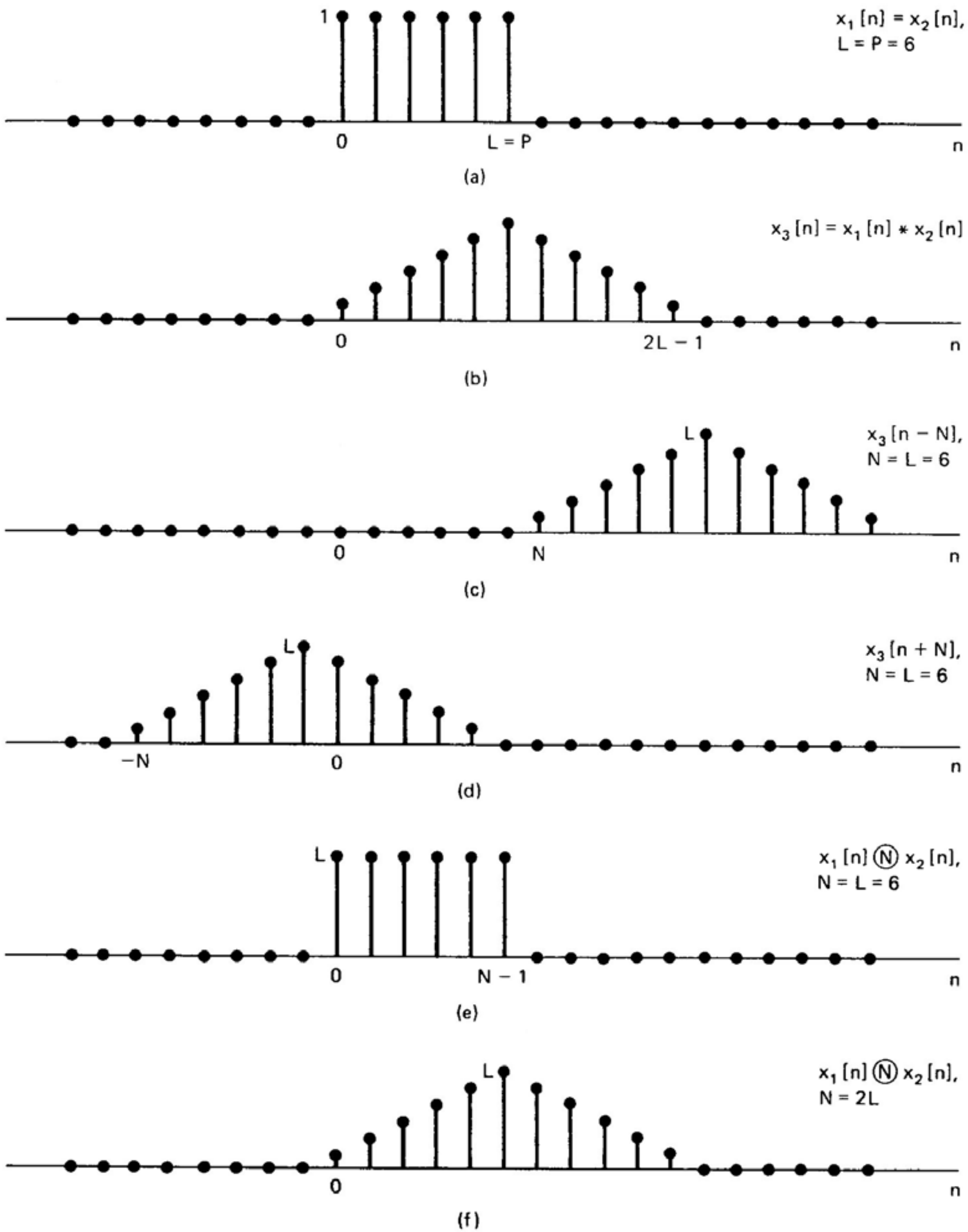

CR, CV and PSD Functions

Definitions:

$$R_{gh}(t_k) = \boldsymbol{E}\{g(t_l)h(t_k + t_l)\} = \lim_{N\to\infty}\frac{1}{N}\sum_{l=0}^{N-1} g(t_l)h(t_k + t_l) = \lim_{T_o\to\infty}\frac{1}{T_o} g(t_k)\otimes h(t_k)$$

$$C_{gh}(t_k) = \boldsymbol{E}\{\{g(t_l) - \overline{g}][h(t_k + t_l) - \overline{h}]\} = \lim_{N\to\infty}\frac{1}{N}\sum_{l=0}^{N-1}[g(t_l) - \overline{g}][h(t_k + t_l) - \overline{h}]$$

$$= \lim_{T_o\to\infty}\frac{1}{T_o} g(t_k)\otimes h(t_k) - \overline{g}\overline{h} = R_{gh}(t_k) - \overline{g}\overline{h}$$

$$P_{gh}(f_m) = \boldsymbol{F}\{R_{gh}(t_k)\} = \lim_{T_o\to\infty}\frac{1}{T_o} G(f_m)H^*(f_m)$$

Computation by FFT:

$$\hat{P}_{gh}(f_m) = \frac{1}{\nu T_o}\sum_{\lambda=1}^{\nu} G_\lambda(f_m)H_\lambda^*(f_m)$$

$$\hat{R}_{gh}(t_k) = \boldsymbol{F}^{-1}\{\hat{P}_{gh}(f_m)\}$$

$$\hat{C}_{gh}(t_k) = \boldsymbol{F}^{-1}\{\hat{P}_{gh}(f_m) - \overline{g}\overline{h}\delta(f_m)\}$$

The DFT in Computers

Subroutines usually assume $\Delta t = 1$ and also ignore T_0.
This requires rescaling as follows:

$$H(f_m) = T_o H_c(m) = N\Delta t H_c(m)$$

$$x(t_k) = g(t_k) * h(t_k) = T_o x_c(t_k) = T_o \boldsymbol{F_c^{-1}}\{G_c(m)H_c(m)\}$$

It also yields: $H_c(0) = \overline{h}$

Subroutines also assume the origin at the left of the record.
This requires changing the phase of the spectrum by $e^{-i2\pi m\Delta f T_o/2} = e^{-i\pi m}$

$$= \cos(m\pi) = (-1)^m$$

$$h(t_k - T_o/2) \leftrightarrow (-1)^m H(f_m)$$

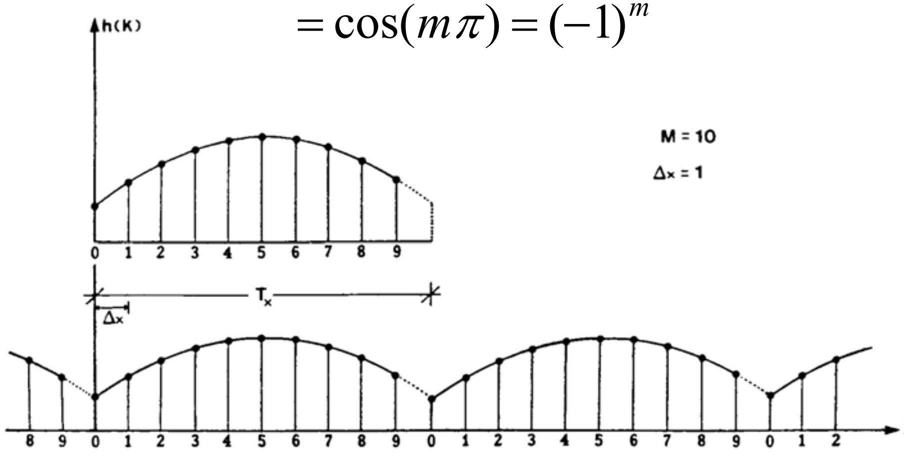

End point of a period must be omitted
(assumed due to periodicity)

The FFT - Flow Graph of Operations for N=4

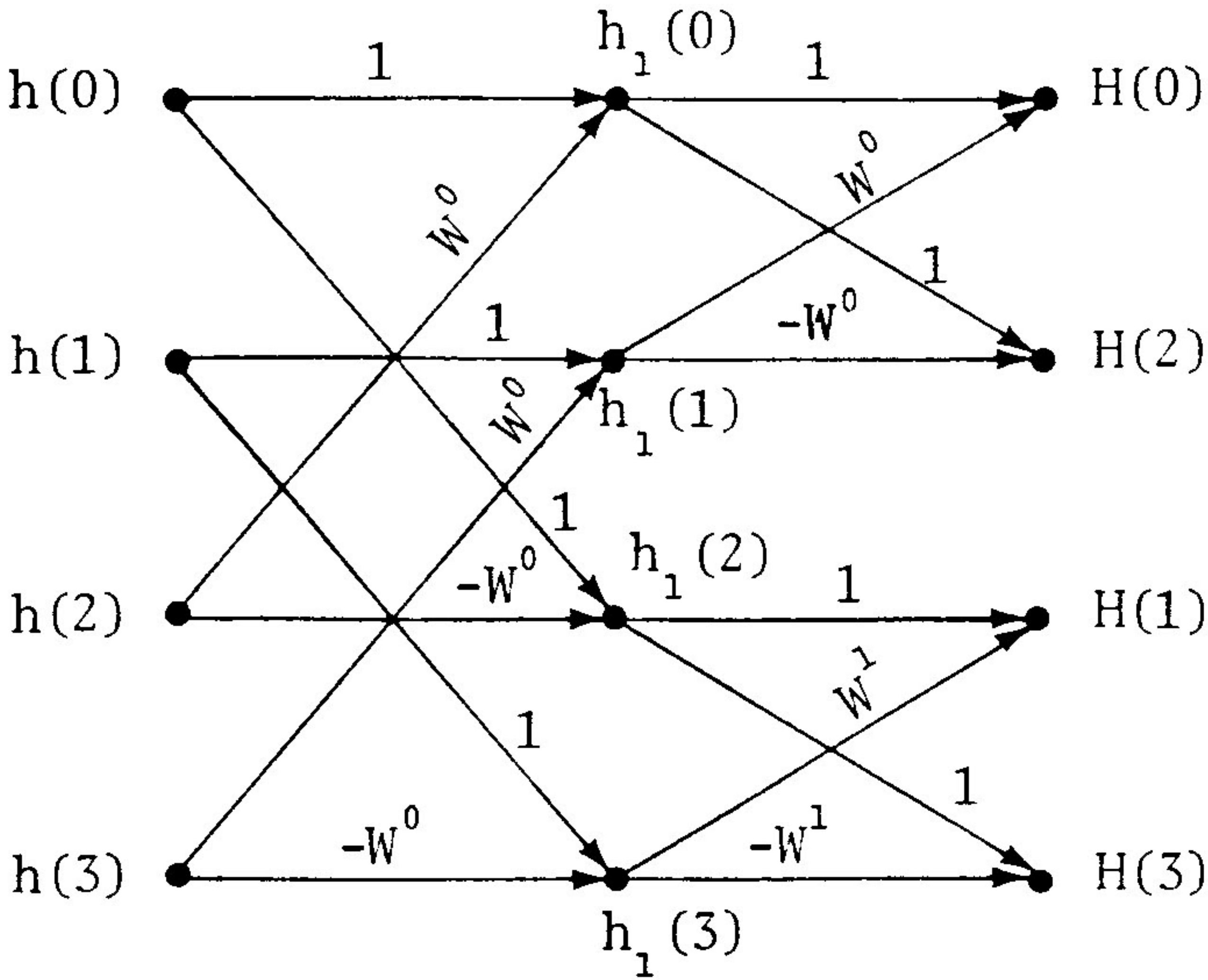

The Two-dimensional DFT

$$H(u_m, v_n) = \sum_{k=0}^{M-1} \sum_{l=0}^{N-1} h(x_k, y_l) e^{-i2\pi(mk/M + nl/N)} \Delta x \Delta y$$

$$h(x_k, y_l) = \sum_{k=0}^{M-1} \sum_{l=0}^{N-1} H(u_m, v_n) e^{i2\pi(mk/M + nl/N)} \Delta u \Delta v$$

SPACE DOMAIN

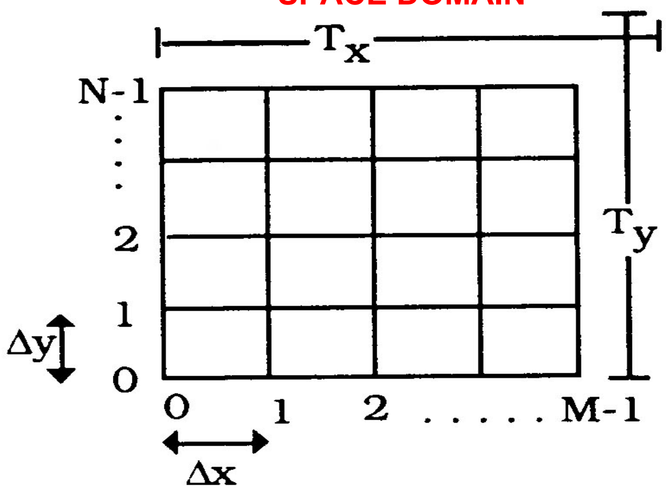

FREQUENCY DOMAIN

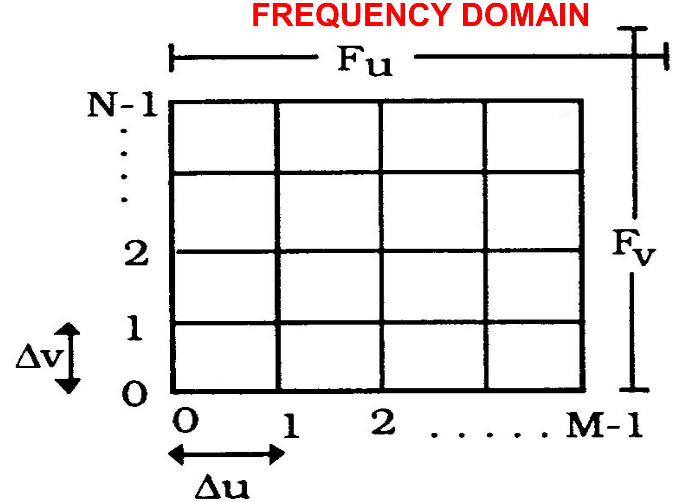

$$\Delta u = \frac{1}{T_y} = \frac{1}{M\Delta x}, \qquad \Delta v = \frac{1}{T_y} = \frac{1}{N\Delta y}$$

$$\Delta x = \frac{1}{F_u} = \frac{1}{M\Delta u} = \frac{1}{2u_N}, \qquad \Delta y = \frac{1}{F_v} = \frac{1}{N\Delta v} = \frac{1}{2v_N}$$

Geoid Undulations by FFT

Geoid Undulations by FFT (1/9)

PLANAR APPROXIMATION OF STOKES'S INTEGRAL

$$N(x_P, y_P) = \frac{1}{2\pi\gamma} \iint_E \frac{\Delta g(x,y)}{\sqrt{(x_p - x)^2 + (y_p - y)^2}} dxdy = \frac{1}{\gamma} \Delta g(x_P, y_P) * l_N(x_P, y_P)$$

$$l_N(x,y) = (2\pi)^{-1}(x^2 + y^2)^{-1/2}$$

FFT: two direct and one inverse Fourier transform

$$N(x,y) = \frac{1}{\gamma} \boldsymbol{F}^{-1}\{\boldsymbol{F}\{\Delta g(x,y)\}\boldsymbol{F}\{l_N(x,y)\}\} = \frac{1}{\gamma} \boldsymbol{F}^{-1}\{\Delta G(u,v) L_N(u,v)\}$$

Geoid Undulations by FFT (2/9)

Point Gravity Anomalies as Input

$$N(x_k, y_l) = \frac{1}{\gamma} \sum_{i=0}^{M-1} \sum_{j=0}^{N-1} \Delta g(x_i, y_j) 1_N (x_k - x_i, y_l - y_j) \Delta x \Delta y$$

FFT: two direct and one inverse Fourier transform

$$l_N(x_k - x_i, y_l - y_j) = \begin{cases} (2\pi)^{-1} [(x_k - x_i)^2 + (y_l - y_j)^2]^{-1/2}, & x_k \neq x_i \text{ or } y_l \neq y_j \\ 0, & x_k = x_i \text{ and } y_l = y_j \end{cases}$$

$$N(x_k, y_l) = \frac{1}{2\pi\gamma} \boldsymbol{F}^{-1} \{ \Delta G(u_m, v_n)\ L_N(u_m, v_n) \}$$

$$L_N(u_m, v_n) = \boldsymbol{F}\{ l_N(x_k, y_l) \} = \sum_{k=0}^{M-1} \sum_{l=0}^{N-1} l_N(x_k, y_l)\, e^{-j 2\pi(mk/M + nl/N)} \Delta x \Delta y$$

$$\Delta G(u_m, v_n) = \boldsymbol{F}\{ \Delta g(x_k, y_l) \} = \sum_{k=0}^{M-1} \sum_{l=0}^{N-1} \Delta g(x_k, y_l)\, e^{-j 2\pi(mk/M + nl/N)} \Delta x \Delta y$$

Geoid Undulations by FFT (3/9)

Mean Gravity Anomalies as Input

$$N(x_k, y_l) = \frac{1}{2\pi\gamma} \sum_{i=0}^{M-1} \sum_{j=0}^{N-1} \overline{\Delta g}(x_i, y_j) \overline{l_N}(x_k - x_i, y_l - y_j)$$

$$\overline{l_N}(x_k, y_l) = \int_{x_k-\Delta x/2}^{x_k+\Delta x/2} \int_{y_l-\Delta y/2}^{y_l+\Delta y/2} \frac{1}{\sqrt{x^2+y^2}} dxdy$$

$$= x\ln(y + \sqrt{x^2+y^2}) + y\ln(x + \sqrt{x^2+y^2}) \Big|_{x_k-\Delta x/2}^{x_k+\Delta x/2} \Big|_{y_l-\Delta y/2}^{y_l+\Delta y/2}$$

FFT: two direct and one inverse Fourier transform

$$N(x_k, y_l) = \frac{1}{2\pi\gamma} \boldsymbol{F}^{-1}\{\boldsymbol{F}\{\overline{\Delta g}(x_k, y_l)\}\boldsymbol{F}\{\overline{l_N}(x_k, y_l)\}\} = \frac{1}{2\pi\gamma} \boldsymbol{F}^{-1}\{\overline{\Delta G}(u_m, v_n)\, \overline{L_N}(u_m, v_n)\}$$

Geoid Undulations by FFT (4/9)

Effects of Planar Approximation - Spherical Corrections

Factors for correcting planar ξ, η, N (or T or ζ) for the Earth's curvature

To avoid long-wavelength errors, the area of local data should not extend to more than several hundreds of kilometers in each direction.

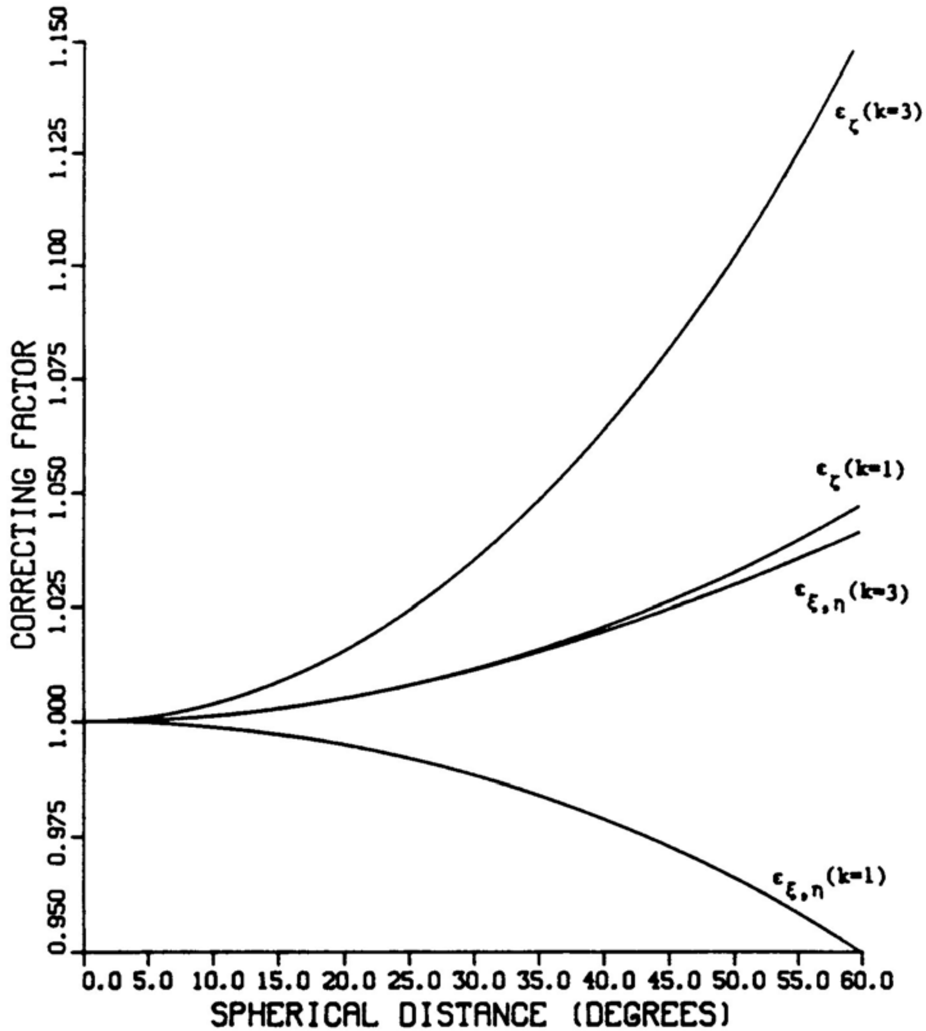

Geoid Undulations by FFT (5/9)

Spherical form of Stokes's Integral

$$N(\varphi_p, \lambda_p) = \frac{R}{4\pi\gamma} \iint_E \Delta g(\varphi, \lambda)\, S(\varphi_p, \lambda_p, \varphi, \lambda)\, \cos\varphi\, d\varphi d\lambda$$

$$N(\varphi_l, \lambda_k) = \frac{R}{4\pi\gamma} \sum_{j=0}^{N-1} \sum_{i=0}^{M-1} \Delta g(\varphi_j, \lambda_i) \cos\varphi_j\, S(\varphi_l, \lambda_k, \varphi_j, \lambda_i)\, \Delta\varphi \Delta\lambda$$

With different approximations of Stokes's kernel function on the sphere, geoid undulations can be evaluated at all gridded points simultaneously by means of either the one-dimensional or the two-dimensional fast Fourier transform

Geoid Undulations by FFT (6/9)

Approximated Spherical Kernel

$$\cos\phi_P \cos\phi \xrightarrow{\text{approximation}} \cos^2\bar{\phi} - \sin^2(\phi_P - \phi)/2$$

$$\sin^2\frac{\psi}{2} = \sin^2\frac{\varphi_P - \varphi}{2} + \sin^2\frac{\lambda_P - \lambda}{2}\cos\varphi_P\cos\varphi$$

$$\sin^2\frac{\psi}{2} \approx \sin^2\frac{\varphi_p - \varphi}{2} + \sin^2\frac{\lambda_p - \lambda}{2}\cos^2\bar{\varphi}$$

$$\approx \sin^2\frac{\varphi_p - \varphi}{2} + \sin^2\frac{\lambda_p - \lambda}{2}\left(\cos^2\bar{\varphi} - \sin^2\frac{\varphi_p - \varphi}{2}\right)$$

$$N(\varphi_l, \lambda_k) = \frac{R}{4\pi\gamma}\sum_{j=0}^{N-1}\sum_{i=0}^{M-1}\Delta g(\varphi_j, \lambda_i)\cos\varphi_j\, S(\varphi_l - \varphi_j, \lambda_k - \lambda_i, \bar{\varphi})\Delta\varphi\Delta\lambda$$

$$= \frac{R}{4\pi\gamma}[\Delta g(\varphi_l, \lambda_k)\cos\varphi_l] * S(\varphi_l, \lambda_k, \bar{\varphi}).$$

$$N(\varphi_l, \lambda_k) = \frac{R}{4\pi\gamma}\boldsymbol{F}^{-1}\{\boldsymbol{F}\{\Delta g(\varphi_l, \lambda_k)\cos\varphi_l\}\boldsymbol{F}\{S(\varphi_l, \lambda_k, \bar{\varphi})\}\}$$

Geoid Undulations by FFT (7/9)

Latitude bands used in the multi-band spherical FFT approach

$$\sin^2\frac{\psi}{2} \approx \sin^2\frac{\varphi_p - \varphi}{2} + \sin^2\frac{\lambda_p - \lambda}{2}\cos\overline{\varphi}_\iota \cos[\overline{\varphi}_\iota - (\overline{\varphi}_\iota - \varphi)]$$

$$\approx \sin^2\frac{\varphi_p - \varphi}{2} + \sin^2\frac{\lambda_p - \lambda}{2}[\cos^2\overline{\varphi}_\iota \cos(\overline{\varphi}_\iota - \varphi) + \cos\overline{\varphi}_\iota \sin\overline{\varphi}_\iota \sin(\overline{\varphi}_\iota - \varphi)]$$

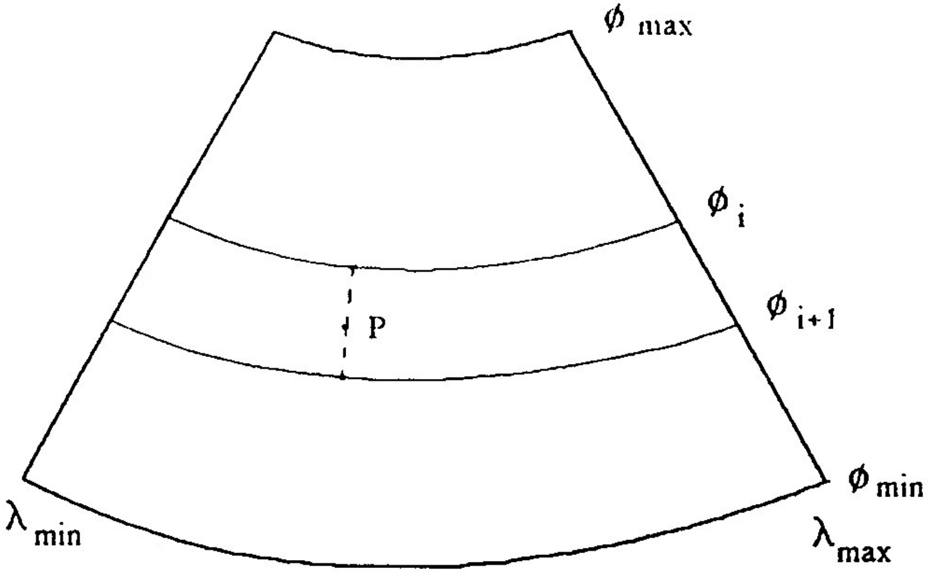

Geoid Undulations by FFT (8/9)

Rigorous Spherical Kernel

$$N(\varphi_l,\lambda_k)=\frac{R}{4\pi\gamma}\sum_{j=0}^{N-1}\Big[\sum_{i=0}^{M-1}\Delta g(\varphi_j,\lambda_i)\cos\varphi_j S(\varphi_l,\varphi_j,\lambda_k-\lambda_i)\Delta\lambda\Big]\ \Delta\varphi, \qquad \varphi_l=\varphi_1,\varphi_2,\ldots,\varphi_N$$

Addition Theorem of DFT

$$N(\varphi_l,\lambda_k)=\frac{R}{4\pi\gamma}\boldsymbol{F}_{\boldsymbol{1}}^{-1}\Big\{\sum_{j=0}^{N-1}\boldsymbol{F}_{\boldsymbol{1}}\{\Delta g(\varphi_j,\lambda_k)\cos\varphi_j\}\boldsymbol{F}_{\boldsymbol{1}}\{S(\varphi_l,\varphi_j,\lambda_k\}\Big\}, \qquad \varphi_l=\varphi_1,\varphi_2,\ldots,\varphi_N$$

The advantage of the 1D spherical FFT approach: it gives exactly the same results as those obtained by direct numerical integration. it only needs to deal with one one-dimensional complex array each time, resulting in a considerable saving in computer memory as compared to the 2D FFT technique discussed before

Geoid Undulations by FFT (9/9)

Computational procedure:

- Subtract effect of GM from Δg (long wavelength)
- Subtract effect of terrain from Δg (short wavelength)
- Use the reduced Δg in the FFT formulas
- Add to the results (reduced co-geoid) the GM effect
- Add to the results (reduced co-geoid) the indirect terrain effects

Edge Effects and Circular Convolution - Zero Padding

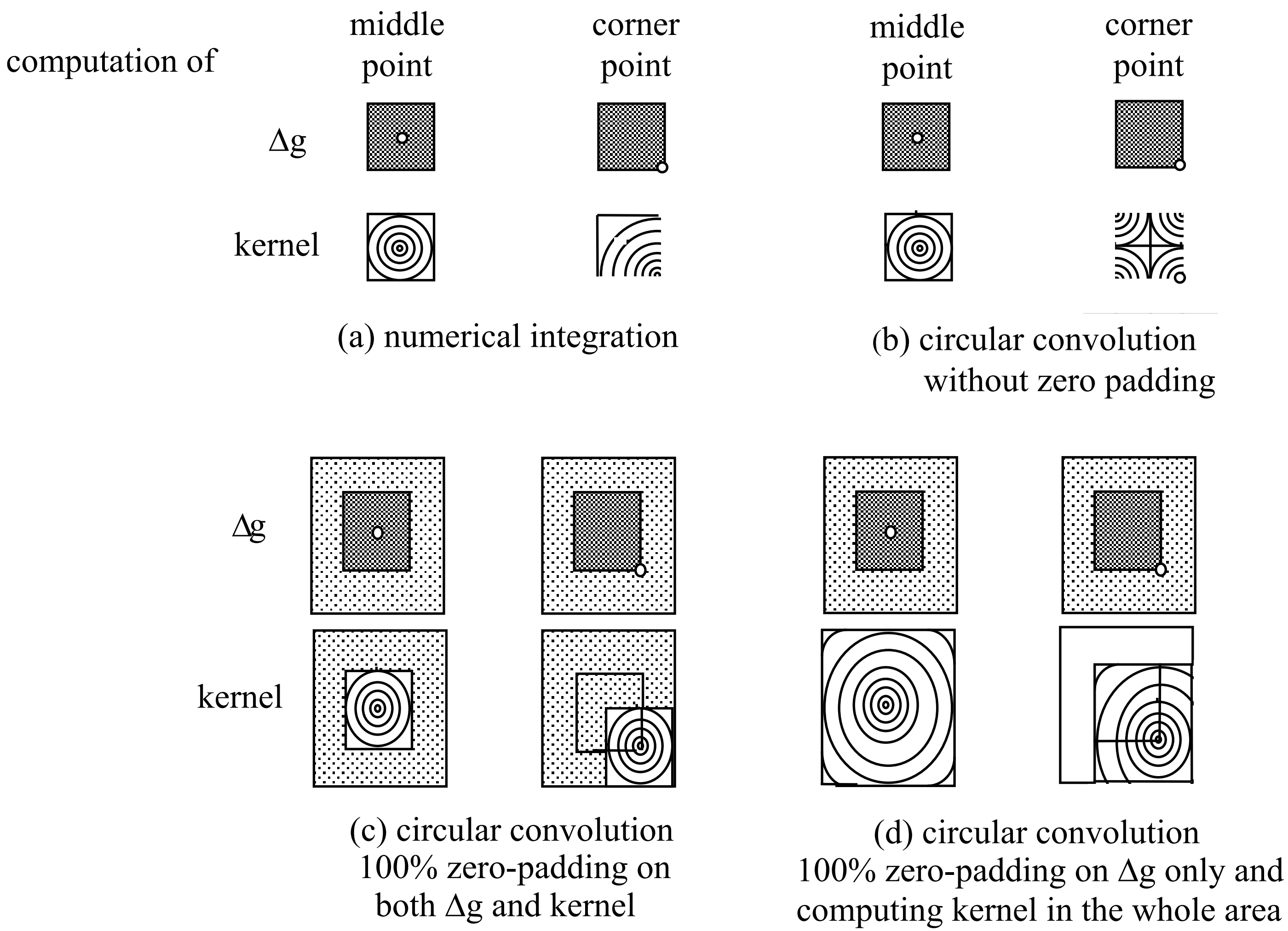

Optimal Spectral Geoid Determination

Error propagation (1/2)

FFT method can use heterogeneous data, provided that they are given on a grid, and can produce error estimates, provided the PSDs (the Fourier transform of the covariance functions) of the data and their noise are known and stationary

$$(\Delta g + n) * s + \varepsilon = N, \qquad s = \frac{l_N}{\gamma}$$

$$\boldsymbol{F}\{N\} = (\boldsymbol{F}\{\Delta g\} + \boldsymbol{F}\{n\})\boldsymbol{F}\{s\} + \boldsymbol{F}\{e\}$$

Multiplying by the complex conjugate of $\boldsymbol{F}\{N\}$ first and then by the complex conjugate of $\boldsymbol{F}\{\Delta g\}$, we get :

$$P_{NN} = P_{ee} + S(P_{\Delta g \Delta g} + P_{nn})S^* = P_{ee} + |S|^2 (P_{\Delta g \Delta g} + P_{nn})$$

$$P_{N\Delta g} = S(P_{\Delta g \Delta g} + P_{nn})$$

No correlation between signal and noise and between input and output noise

S is the spectrum of s, and $P_{\Delta g \Delta g}$ is the PSD of the gravity anomalies

Error Propagation (2/2)

$$\boldsymbol{F}\{N\} = \boldsymbol{F}\{\Delta g\}\boldsymbol{F}\{s\} = P_{N\Delta g}(P_{\Delta g\Delta g} + P_{nn})^{-1}\boldsymbol{F}\{\Delta g\}$$ spectral form

$$S = P_{N\Delta g}(P_{\Delta g\Delta g} + P_{nn})^{-1} = S_0(1 + \frac{P_{nn}}{P_{\Delta g\Delta g}})^{-1}, \qquad S_0 = \frac{P_{N\Delta g}}{P_{\Delta g\Delta g}}$$

$$\hat{\boldsymbol{N}} = \boldsymbol{C}_{N\Delta g}(\boldsymbol{C}_{\Delta g\Delta g} + \boldsymbol{C}_{nn})^{-1}\Delta\boldsymbol{g}$$ → collocation form

$$P_{ee} = P_{NN} - P_{N\Delta g}(P_{\Delta g\Delta g} + P_{nn})^{-1}P_{\Delta gN} = |S_0|^2 P_{\Delta g\Delta g}[1 - (1 + \frac{P_{nn}}{P_{\Delta g\Delta g}})^{-1}]$$ spectral form

$$\boldsymbol{C}_{ee} = \boldsymbol{C}_{NN} - \boldsymbol{C}_{N\Delta g}(\boldsymbol{C}_{\Delta g\Delta g} + \boldsymbol{C}_{nn})^{-1}\boldsymbol{C}_{N\Delta g}^{T}$$ → collocation form

Other Applications of FFT

Application 1: Terrain Corrections by FFT (1/2)

Conventional Computation of TC

- Single point computation
- Numerical integration: summation of contributions of compartments (prisms)
- Time consuming: $t \sim N^2$

FFT Computation of TC

- Convolution integral
- Homogeneous TC coverage for BVPs
- Height files on regular grid
- Need for faster methods → FFT approach ideal
- Reduced computation time: $t \sim N \log N$
- Handling of large amounts of gridded data
- Spectral analysis; covariance functions

DATA: gridded h (and ρ)

OBJECTIVE: Rigorous and fast evaluation of TC integral

Terrain Corrections by FFT(2/2)

$$c(x_P,y_P)=\frac{1}{2}k\rho\iint_E \frac{h^2(x,y)-h^2(x_P,y_P)}{[(x_P-x)^2+(x_P-x)^2]^{3/2}}dxdy$$

$$-h(x_P,y_P)k\rho\iint_E \frac{h(x,y)-h(x_P,y_P)}{[(x_P-x)^2+(x_P-x)^2]^{3/2}}dxdy$$

$$=\frac{1}{2}k\rho\{h^2(x_P,y_P)*l_c(x_P,y_P)-h^2(x_P,y_P)[o(x_P,y_P)*l_c(x_P,y_P)]$$

$$-2h(x_P,y_P)[h(x_P,y_P)*l_c(x_P,y_P)-h(x_P,y_P)[o(x_P,y_P)*l_c(x_P,y_P)]]\}$$

where $l_c(x,y)=(x^2+y^2)^{-3/2}$ and $o(x,y)=1$

PROCEDURE

- Transform h, $h_2=h^2$, o, l_c to H, H_2, O, L_c (direct FFT) and form $H\,L_c$, $H_2\,L_c$, $O\,L_c$
- Transform $H\,L_c$, $H_2\,L_c$, $O\,L_c$ to $h*l_c$, h_2*l_c, $o*l_c$ (inverse FFT)
- Multiply and add/subtract terms as needed

$$c(x,y)=\frac{1}{2}k\rho\{\boldsymbol{F}^{-1}\{H_2(u,v)L_c(u,v)\}-h^2(x,y)\boldsymbol{F}^{-1}\{O(u,v)L_c(u,v)\}$$

$$-2h(x,y)[\boldsymbol{F}^{-1}\{H(u,v)L_c(u,v)\}-h(x,y)\boldsymbol{F}^{-1}\{O(u,v)L_c(u,v)\}]\}$$

Application 2:
Stokes and Vening Meinesz on the plane (1/2)

$$N(x_p, y_p) = \frac{1}{2\pi\gamma} \iint_E \Delta g(x,y) \frac{1}{\left[(x_p - x)^2 + (y_p - y)^2\right]^{1/2}} = \frac{1}{2\pi\gamma} \Delta g(x_p, y_p) * l_N(x_p, y_p)$$

$$l_N(x,y) = (x^2 + y^2)^{-1/2}$$

$$\begin{Bmatrix} \xi(x_p, y_p) \\ \eta(x_p, y_p) \end{Bmatrix} = \begin{Bmatrix} -\partial N(x_p, y_p)/\partial y_P \\ -\partial N(x_p, y_p)/\partial x_P \end{Bmatrix} = -\frac{1}{2\pi\gamma} \begin{Bmatrix} \Delta g(x_p, y_p) * \partial l_N(x_p, y_p)/\partial y_P \\ \Delta g(x_p, y_p) * \partial l_N(x_p, y_p)/\partial y_P \end{Bmatrix}$$

$$= -\frac{1}{2\pi\gamma} \Delta g(x_p, y_p) * \begin{Bmatrix} l_\xi(x_p, y_p) \\ l_\eta(x_p, y_p) \end{Bmatrix}$$

$$\begin{Bmatrix} l_\xi(x,y) \\ l_\eta(x,y) \end{Bmatrix} = -\begin{Bmatrix} \partial l_N(x,y)/\partial y \\ \partial l_N(x,y)/\partial x \end{Bmatrix} = (x^2 + y^2)^{-3/2} \begin{Bmatrix} y \\ x \end{Bmatrix}$$

$$\begin{Bmatrix} \xi(x_p, y_p) \\ \eta(x_p, y_p) \end{Bmatrix} = \frac{1}{2\pi\gamma} \iint_E \Delta g(x,y) \frac{1}{\left[(x_p - x)^2 + (y_p - y)^2\right]^{3/2}} \begin{Bmatrix} y_p - y \\ x_p - x \end{Bmatrix} dxdy$$

Stokes and Vening Meinesz on the plane (2/2)

Since $L_N(u,v) = \boldsymbol{F}\{l_N(x,y)\} = \boldsymbol{F}\left\{(x^2+y^2)^{-1/2}\right\} = (u^2+v^2)^{1/2}$

$$\begin{Bmatrix} l_\xi(x,y) \\ l_\eta(x,y) \end{Bmatrix} = -\begin{Bmatrix} \partial l_N(x,y)/\partial y \\ \partial l_N(x,y)/\partial x \end{Bmatrix}$$

then

$$\boldsymbol{F}\begin{Bmatrix} \xi(x,y) \\ \eta(x,y) \end{Bmatrix} = -\frac{1}{2\pi\gamma}\Delta G(u,v)\begin{Bmatrix} 2\pi iu \\ 2\pi iv \end{Bmatrix} L_N(u,v)$$

$$N(x,y) = \frac{1}{2\pi\gamma}\boldsymbol{F}^{-1}\left\{\Delta G(u,v)\frac{1}{(u^2+v^2)^{1/2}}\right\}$$

High-frequency attenuation (integration)

$$\begin{Bmatrix} \xi(x,y) \\ \eta(x,y) \end{Bmatrix} = -\frac{1}{\gamma}\boldsymbol{F}^{-1}\begin{Bmatrix} \Delta G(u,v)\dfrac{iv}{(u^2+v^2)^{1/2}} \\ \Delta G(u,v)\dfrac{iu}{(u^2+v^2)^{1/2}} \end{Bmatrix}$$

High-frequency amplification (differentiation)

Application 3: Analytical Continuation

Upward continuation from $h=0$ to $h=z_0$

$$\Delta g(x_P, y_P, z_0) = \frac{1}{2\pi}\iint_E \Delta g(x,y,0)\frac{z_0}{[(x_P-x)^2+(y_P-y)^2+z_0^2]^{3/2}}dxdy$$

$$= \Delta g(x_P, y_P, 0) * l_u(x_P, y_P, z_0), \qquad l_u(x,y,z_0) = \frac{z_0}{2\pi[(x^2+y^2+z_0^2]^{3/2}}$$

$$= \boldsymbol{F}^{-1}\{\boldsymbol{F}\{\Delta g(x_P, y_P, 0)\}\boldsymbol{F}\{l_u(x_P, y_P, z_0)\}\}$$

Analytical spectrum of l_u: $\boldsymbol{F}\{l_u(x_P, y_P, z_0)\} = L_u(u,v,z_0) = e^{-2\pi z_0 (u^2+v^2)^{1/2}}$

High-frequency attenuation

Downward continuation from $h=z_0$ to $h=0$

$$\Delta g(x_P, y_P, 0) = \boldsymbol{F}^{-1}\{\tfrac{\boldsymbol{F}\{\Delta g(x_P, y_P, z_0)\}}{\boldsymbol{F}\{l_u(x_P, y_P, z_0)\}}\} = \boldsymbol{F}^{-1}\{\boldsymbol{F}\{\Delta g(x_P, y_P, z_0)\}\boldsymbol{F}\{l_d(x_P, y_P, z_0)\}\}$$

Analytical spectrum of l_d: $\boldsymbol{F}\{l_d(x_P, y_P, z_0)\} = 1/L_u(u,v,z_0) = e^{2\pi z_0 (u^2+v^2)^{1/2}}$

High-frequency amplification

Application 4: Interpolation by FFT

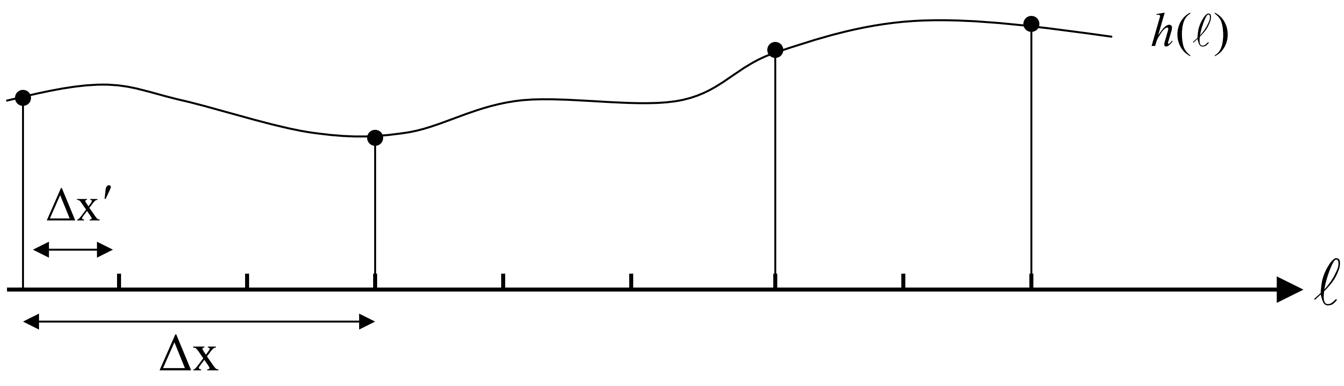

- Want to interpolate with spacing Δx'= Δx / L
- Zeros are filled at L-1 points between the initial pairs of sampled values

$$g(\ell) = \begin{cases} h(1/L), & \ell = 0 \le L \le 2L \\ 0, & elsewhere \end{cases} \qquad G(m) = H(mL) \quad includes\ m > \pm\frac{1}{L}$$

- Filter out higher frequencies, so that

$$-\frac{1}{L} \le m \le \frac{1}{L} \qquad G_1(m) = \begin{cases} c \cdot H(mL), & -\frac{1}{L} \le m \le \frac{1}{L} \\ 0, & elsewhere \end{cases}$$

- Match initial amplitudes

$$g_1(0) = \frac{c}{L} h(0) \quad \rightarrow \ c = L \ \rightarrow g_1(\ell) = F^{-1}\{G_1(m)\}$$

Concluding Remarks

Concluding Remarks

- Spectral methods can efficiently handle large amounts of gridded data and give results on all grid points simultaneously → indispensable for geoid computations
- Problems that affect the accuracy of the results: aliasing, leakage, singularity of the kernel functions at the origin, proper handling of mean and point data → common to all methods using the same data
- Problems unique to spectral methods:
  - Phase shifting
  - Edge effects and circular convolution
  - Planar approximation
- Drawbacks of FFT-based spectral techniques
  - Gridded data ONLY as input
  - Computer memory
  - Fast error propagation possible only with stationary noise

Matching the Gravimetric Geoid to the GPS-Levelling Undulations

Georgia Fotopoulos
gfotopou@ucalgary.ca

Department of Geomatics Engineering
University of Calgary

Contents

- Introduction to problem
- Why combine h, H and N?
- Semi-automated parametric model testing procedure
  - classical empirical approach
  - cross-validation
  - measures of goodness of fit
  - testing parameter significance
- Examples
- Summary

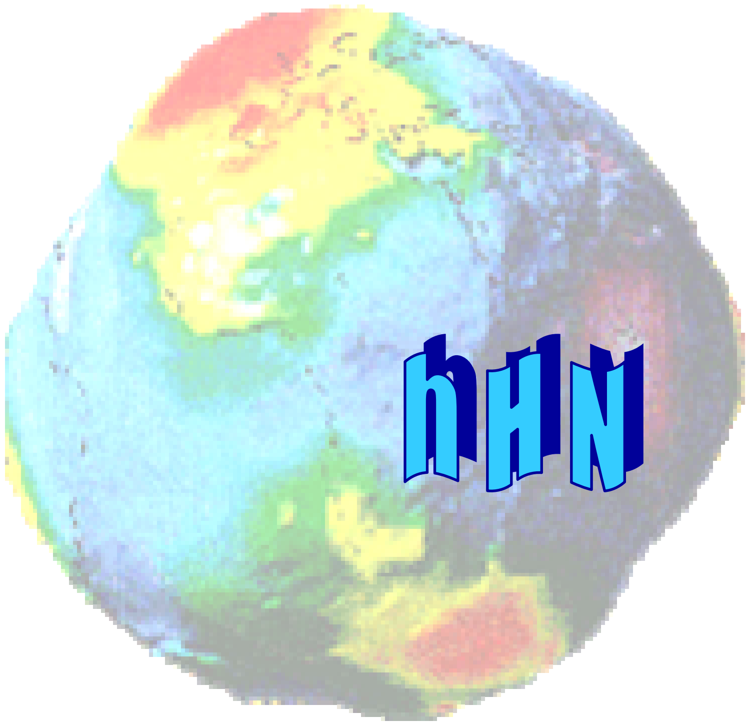

Introduction

- Traditional means for establishing vertical control (**H**): spirit-levelling
  - costly
  - labourious
  - inefficient, difficult in remote areas, mountainous terrain, over large regions

- With advent of satellite-based global positioning systems (GPS) 3D positioning has been revolutionized

h – **H** – **N** = 0

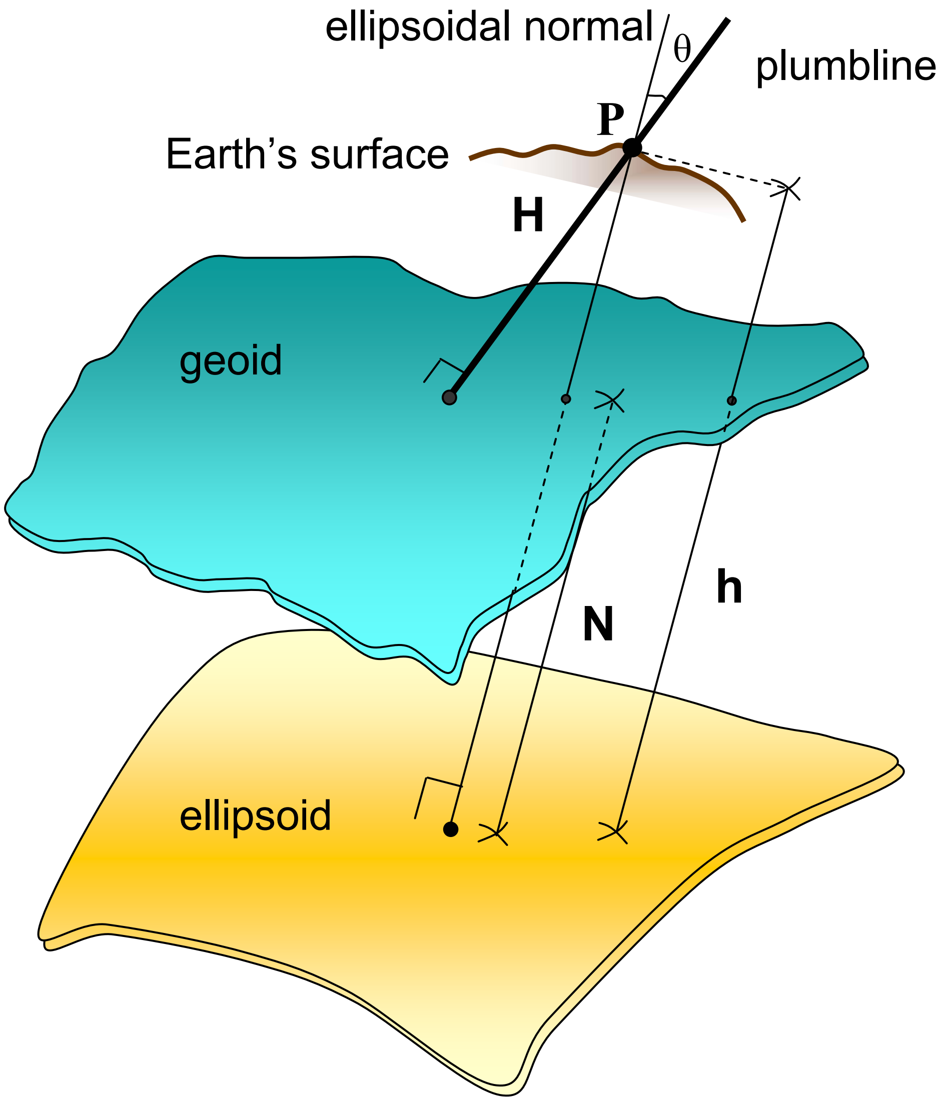

Why combine h, H and N?

- modernize regional vertical datums
- unify/connect national regional datums between neighbouring countries
- transform between different types of height data (GPS-levelling)
- refine and test existing gravimetric geoid models
- better understanding of data error sources
  - calibrate geoid error model
  - assess noise in GPS heights, test a-priori error measures
  - evaluate levelling precision, test a-priori error values

- Other applications: sea level change monitoring, post-glacial rebound studies, etc.

Introduction (continued)

Factors that cause discrepancies when combining heterogeneous heights:

- random errors in the derived heights *h*, *H*, and *N*
- datum inconsistencies inherent among the height types
- systematic effects and distortions (long-wavelength geoid errors, poorly modelled GPS errors and over-constrained levelling network adjustments)
- assumptions/theoretical approximations made in processing observed data (neglecting sea surface topography or river discharge corrections at tide gauges)
- approximate or inexact normal/orthometric height corrections
- instability of reference station monuments over time (geodynamic effects, land uplift/subsidence)

Problem Formulation

Standard practice: Use of a corrector surface to model the datum discrepancies and systematic effects when combining GPS, geoid and orthometric heights

Theory: $h_i - H_i - N_i = 0 \quad \rightarrow \quad N_i^{GPS/levelling} = N_i$

Practice: $h_i - H_i - N_i = l_i \quad \rightarrow \quad N_i^{GPS/levelling} \neq N_i$

Model: $l_i = h_i - H_i - N_i = \mathbf{a}_i^{\mathrm{T}}\mathbf{x} + v_i$

residuals

parametric model

GNSS-Levelling

– Development of corrector surface models to be used with GPS and gravimetric geoid models for GPS-Levelling

$$H_p = h_p - N_p - \mathbf{a}_p^T \hat{\mathbf{x}}$$

corrector surface

known height data

orthometric height at new point

Data

GPS: $h_i, \Delta h_{ij}$ Orthometric heights: $H_i, \Delta H_{ij}$ Geoid model: $N_i, \Delta N_{ij}$

Prediction surface $\rightarrow$ aim is to derive a surface from data which is to be applied to new data

Semi-automated Parametric Model Testing Procedure

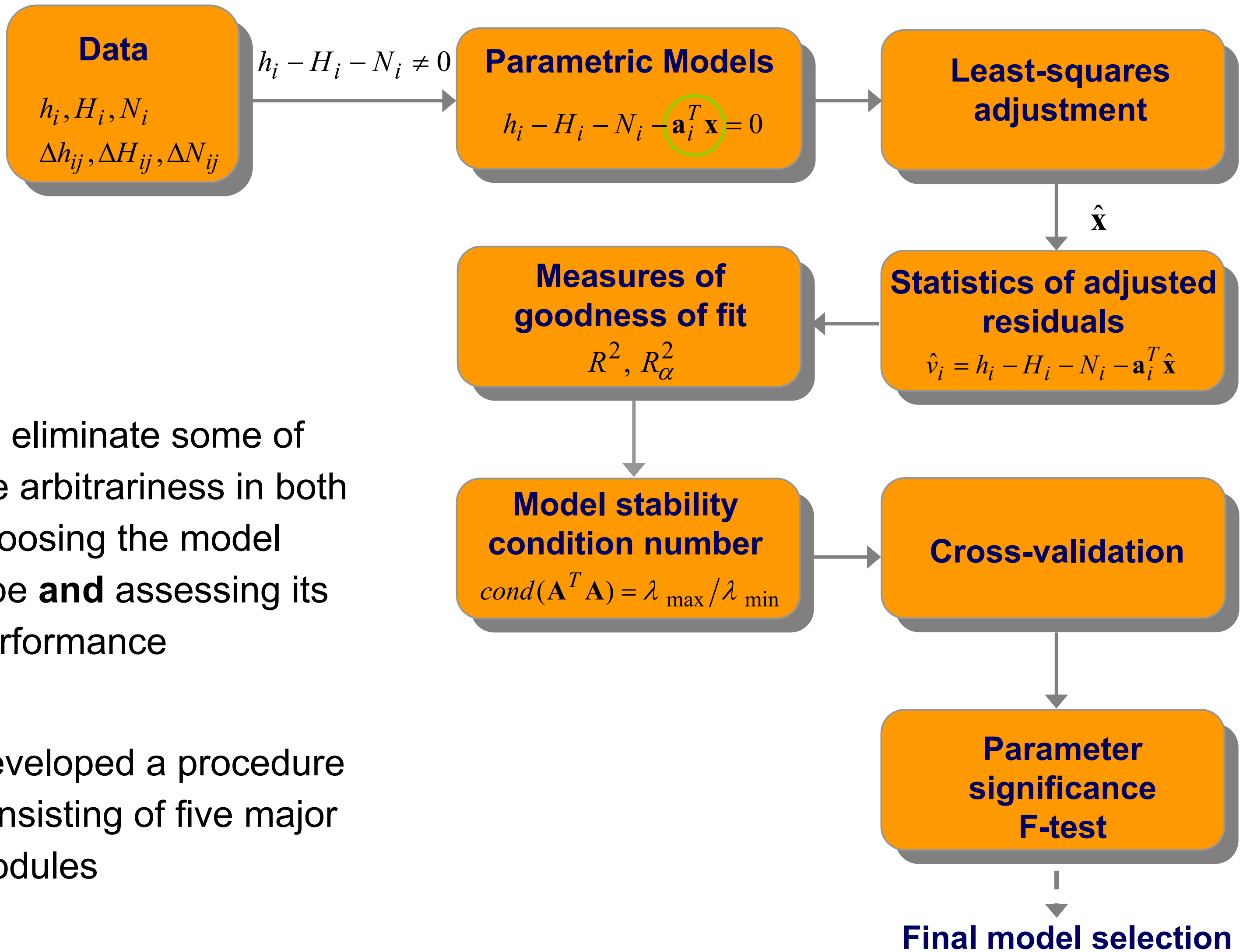

- To eliminate some of the arbitrariness in both choosing the model type **and** assessing its performance
- Developed a procedure consisting of five major modules

Parametric Surface Model Selection

Parametric Models

$$h_i - H_i - N_i - a_i^T x = 0$$

- Selection of analytical model suffers from a degree of arbitrariness *(Why?)*
  - type of model (i.e. polynomial)
  - type of base functions (i.e. trigonometric)
  - number of coefficients
- Need statistical tools to
  - assess choices made
  - compare different models
- Factors for model selection/analysis may vary if
  - nested models
  - orthogonal vs. non-orthogonal models

No straightforward answer, data dependent (geometry)

Classic Empirical Approach

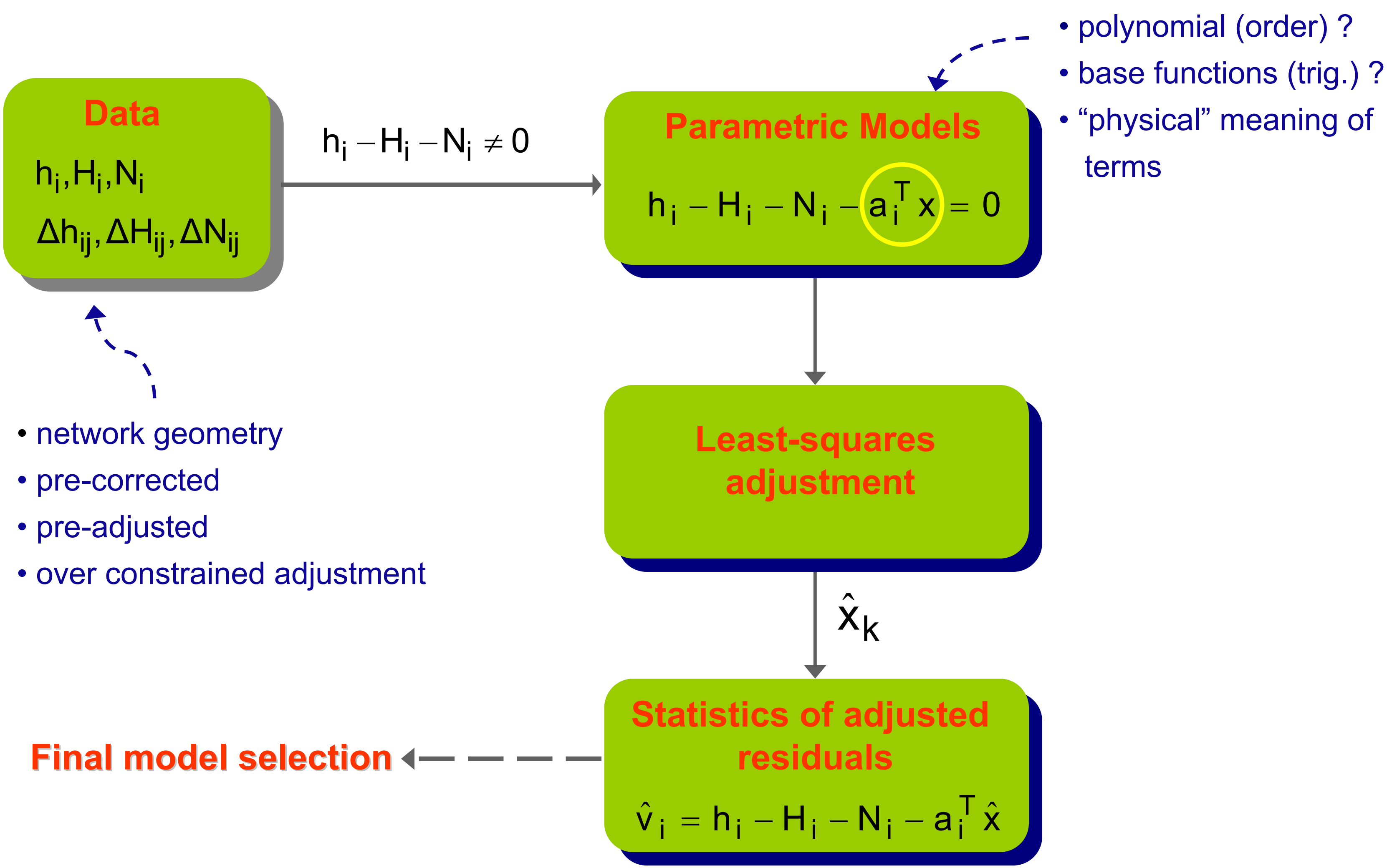

Cross Validation

Cross-validation (empirical approach)

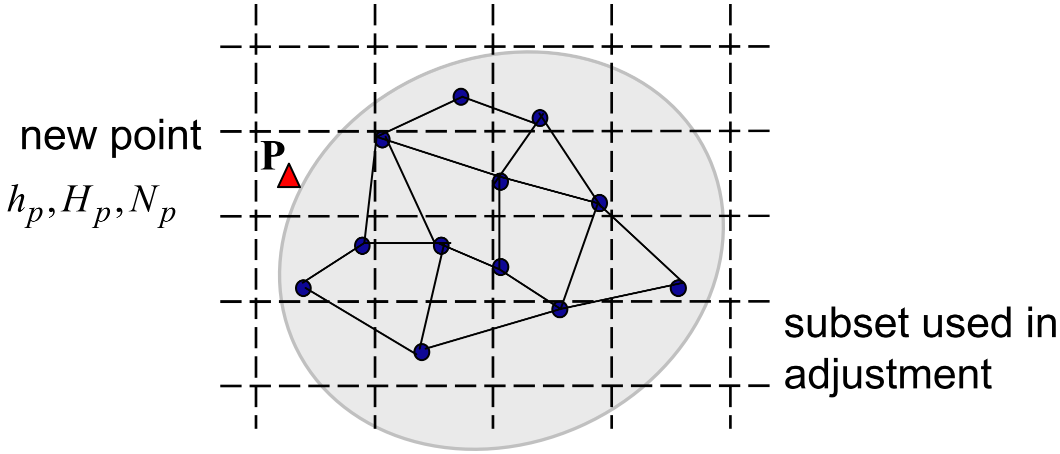

$\mathbf{a}_p^T \hat{\mathbf{x}}$

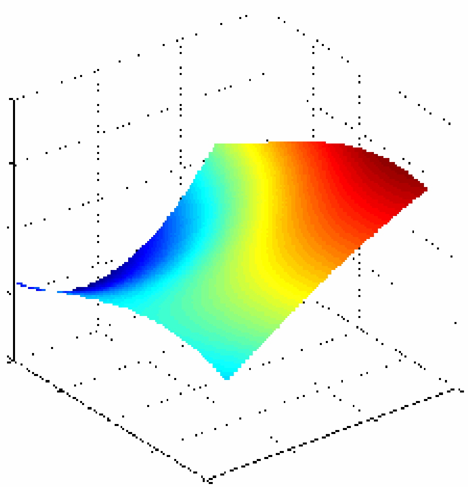

$$\Delta\hat{v}_p = h_p - H_p - N_p - \mathbf{a}_p^T \hat{\mathbf{x}}$$

Repeat for each point and compute:

$$\frac{1}{n}\sum_{i=1}^{n}\sqrt{\mu_i^2 + \sigma_i^2}$$

Measures of Goodness of Fit

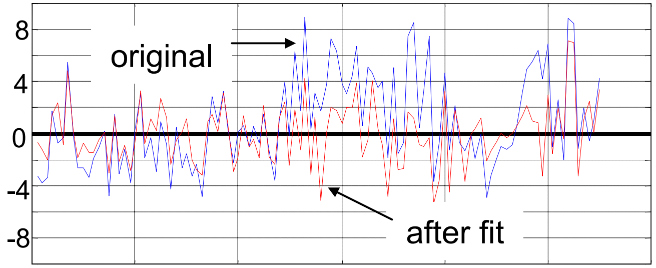

Statistics of adjusted residuals

$$\hat{v}_i = h_i - H_i - N_i - a_i^T \hat{x}$$

Coefficient of determination

R^2

$$R^2 = 1 - \frac{\sum_{i=1}^{n} (\ell_i - \hat{v}_i)^2}{\sum_{i=1}^{n} (\ell_i - \overline{\ell}_i)^2}$$

$$\ell_i = h_i - H_i - N_i$$

n … # of observations

Adjusted coefficient of determination

$\overline{R}^2$

$$\overline{R}^2 = 1 - \frac{\left[\sum_{i=1}^{n} (\ell_i - \hat{v}_i)^2\right] / (n-m)}{\left[\sum_{i=1}^{n} (\ell_i - \overline{\ell}_i)^2\right] / (n-1)}$$

m … # of parameters

Testing Parameter Significance

Reasons for reducing the number of model parameters

- Simplicity, computational efficiency
- Over-parameterization (i.e. high-degree trend models)

  → unrealistic extrema in data voids where control points are missing
- Unnecessary terms may bias other parameters in model

  → hinders capability to assess model performance

Parameter Significance → Need for automated selection process

Stepwise Procedures

Backward Elimination Procedure

- Start with highest order model
- Eliminate less-significant terms one-by-one (or several at once)
- *Criteria* for determining parameter deletion
  - Partial F-test
  - Level of significance, α
  - **Problem:** correlation between parameters

nested
models
only

Forward Selection Procedure

- Start with simple model
- Add parameter with the highest coefficient of determination (or partial F-value)

Stepwise Procedure

- Combination of backward elimination and forward selection procedures
- Starts with no parameters and selects parameters one-by-one (or several)
- After inclusion, examine every parameter for significance (partial F-test)

Stepwise Procedure

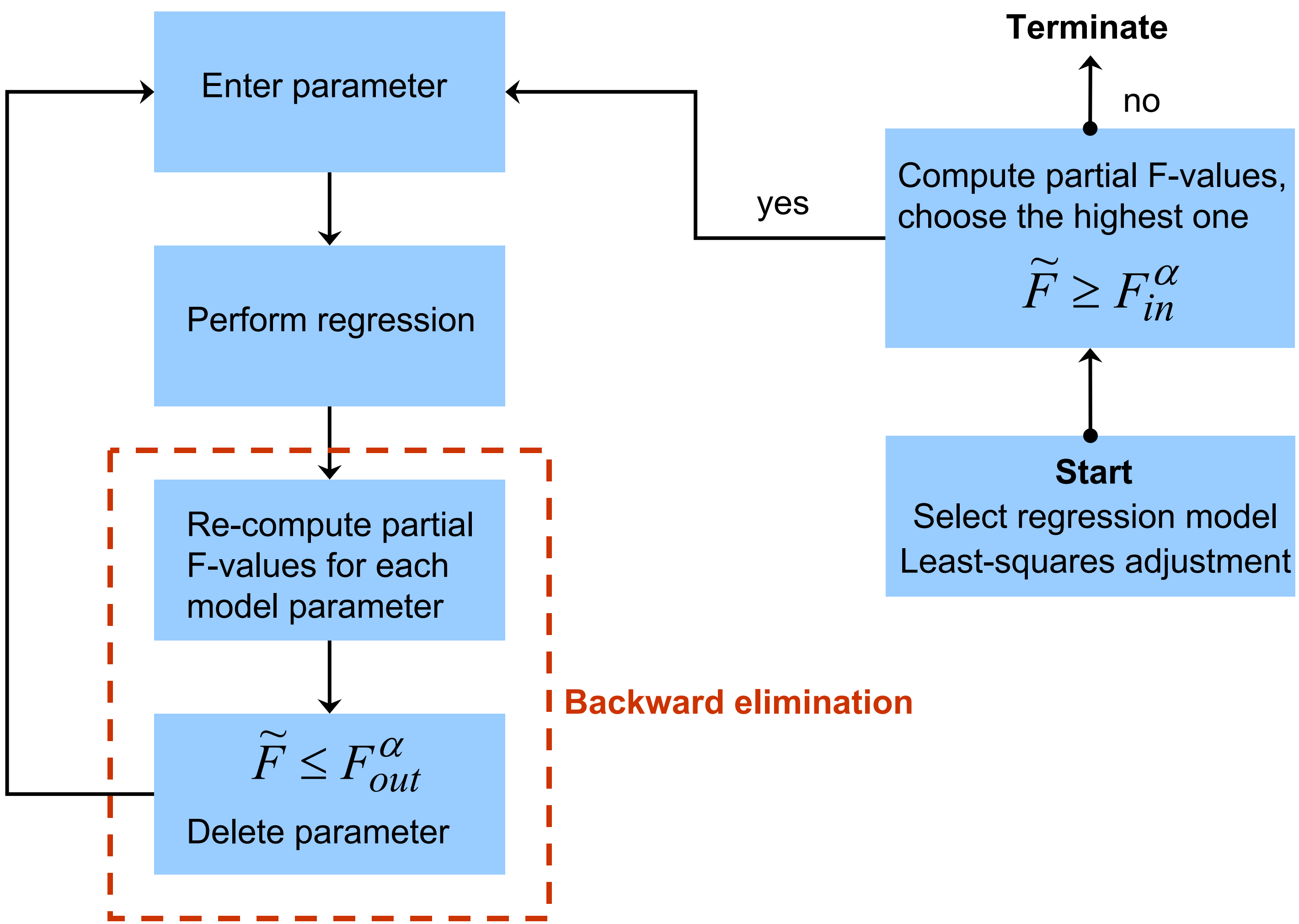

Testing Parameter Significance

- Statistical tests are more powerful in pointing out inappropriate models rather than establishing model validity
- Test if a set of parameters in the model is significant or not:

$$x = \begin{bmatrix} x_{(I)} \\ x_I \end{bmatrix}$$

I … set of parameters tested

(I) … remaining parameters (complement)

hypothesis $H_0 : x_I = 0 \quad \text{vs} \quad H_a : x_I \neq 0$

test statistic $$\tilde{F} = \frac{\hat{x}_I Q_{\hat{x}_I}^{-1} \hat{x}_I}{k\hat{\sigma}^2}$$

k ……… number of 'tested' terms

$Q_{\hat{x}_I}$ …… submatrix of $Q = N^{-1}$

criteria $\tilde{F} \leq F_{k,f}^{\alpha}$ H_0 accepted ✓

Examples - Switzerland

- 111 stations in **Switzerland**
- 343 km × 212 km region
- Form 'residuals':

$$\ell_i = h_i - H_i - N_i$$

Statistics of residuals before fit

min	-4.9 cm
max	19 cm
mean	1.1 cm
std	3.8 cm
rms	3.9 cm

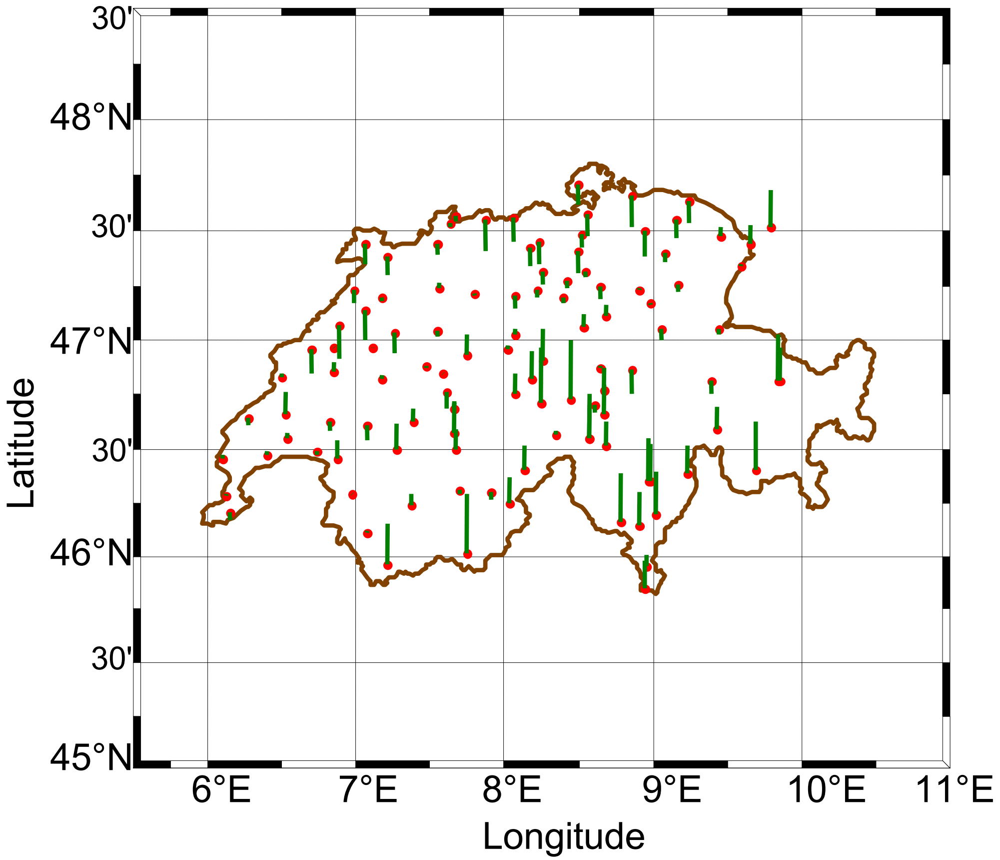

GPS on Benchmarks (and residuals)

Examples - Canada

- 63 stations in **Southern British Columbia** & **Alberta**
- 495 km × 334 km region
- Form 'residuals':

$$\ell_i = h_i - H_i - N_i$$

Stats of residuals before fit

min	-17.1 cm
max	25.2 cm
mean	4.5 cm
std	8.1 cm
rms	9.3 cm

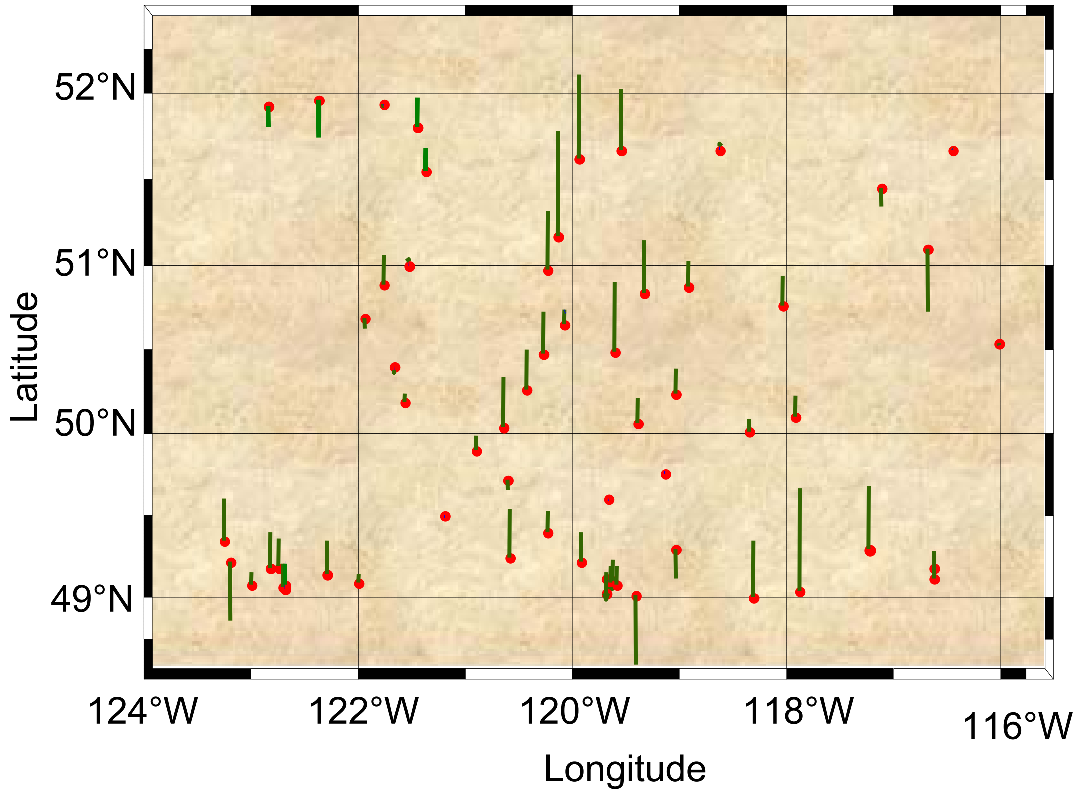

GPS on Benchmarks (and residuals)

Examples of Analytical Models

Nested bilinear polynomial series

$1 \quad d\varphi \quad d\lambda \quad d\varphi d\lambda \quad d\varphi^2 \quad d\lambda^2 \quad d\varphi^2 d\lambda \quad d\varphi d\lambda^2 \quad d\varphi^3 \quad d\lambda^3 \quad d\varphi^2 d\lambda^2 \quad d\varphi^3 d\lambda \quad d\varphi d\lambda^3 \quad d\varphi^4 \quad d\lambda^4$

Classic trigonometric-based polynomial fits

$1 \quad \cos\varphi\cos\lambda \quad \cos\varphi\sin\lambda \quad \sin\varphi$

$1 \quad \cos\varphi\cos\lambda \quad \cos\varphi\sin\lambda \quad \sin\varphi \quad \sin^2\varphi$

Differential similarity transformation

$$\cos\varphi\cos\lambda \quad \cos\varphi\sin\lambda \quad \sin\varphi \quad \frac{\sin\varphi\cos\varphi\sin\lambda}{W} \quad \frac{\sin\varphi\cos\varphi\cos\lambda}{W} \quad \frac{1-f^2\sin^2\varphi}{W} \quad \frac{\sin^2\varphi}{W}$$

where, $W = \sqrt{1-e^2\sin^2\varphi}$

Analytical Models

4th order polynomial

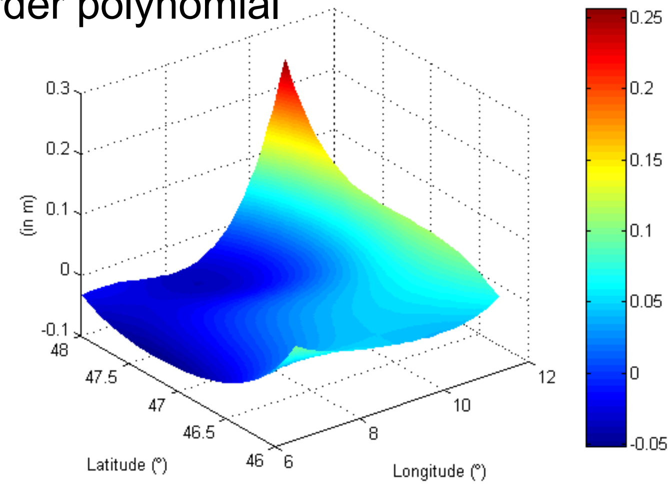

3rd order

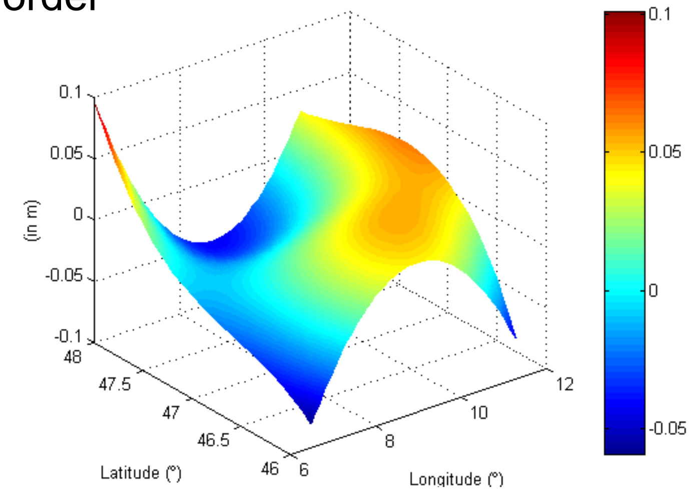

2nd order

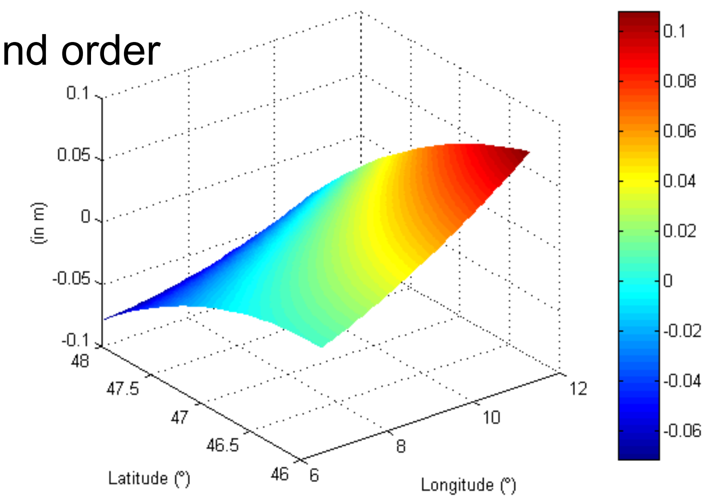

1st order

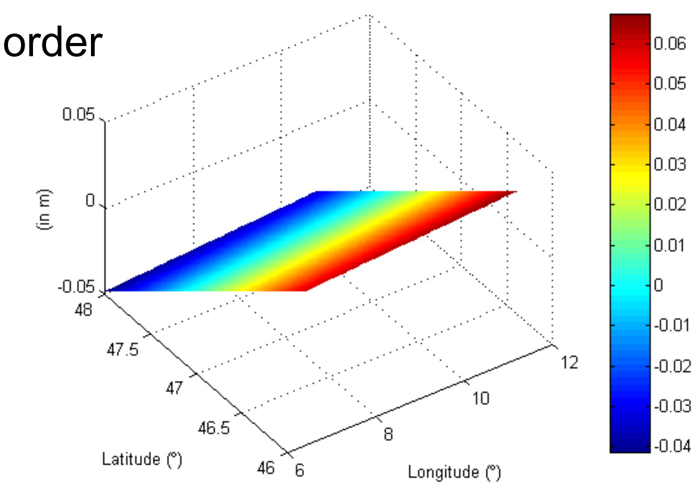

More Analytical Models

Classic 4-parameter

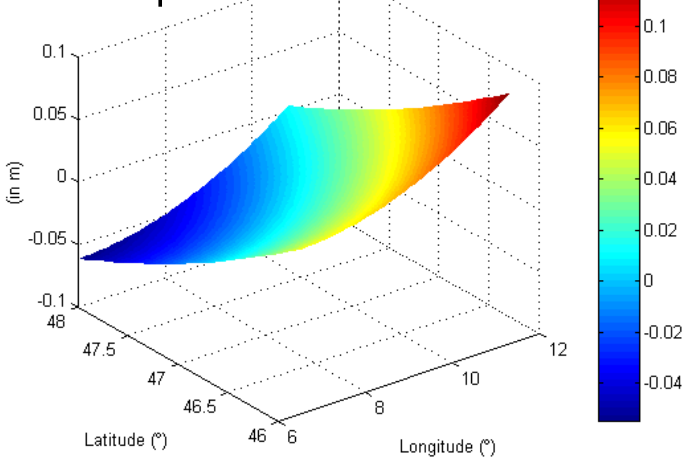

Classic 5-parameter

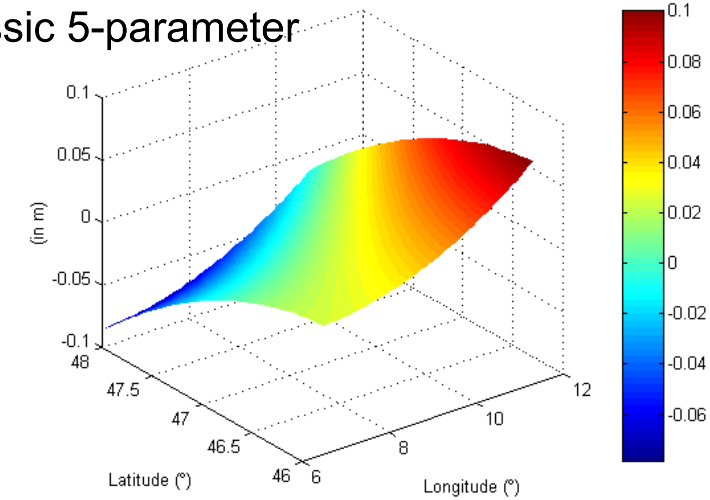

7-parameter differential similarity

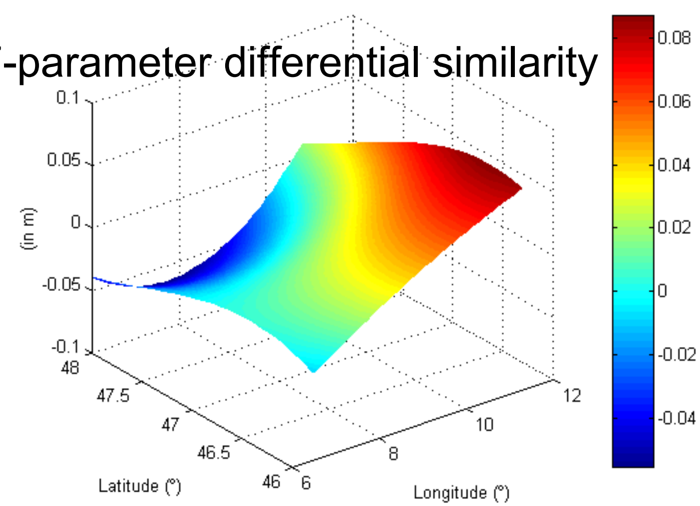

Notes

– all values shown in m

– GPS BMs in Switzerland used

– Full models shown (no parameters omitted)

Example - Coefficient of Determination

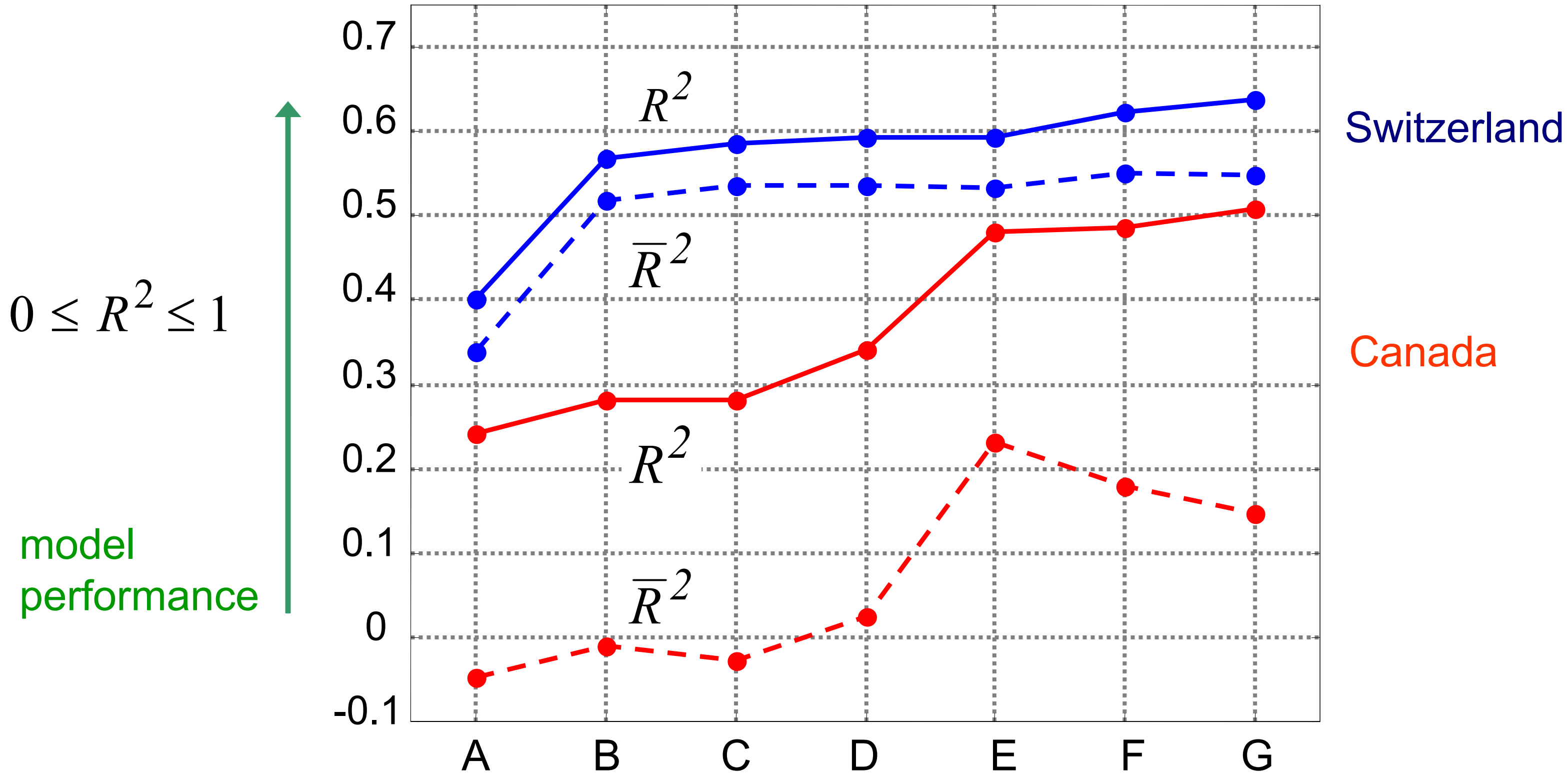

A 1st order polynomial
B Classic 4-parameter
C Classic 5-parameter
D 2nd order polynomial
E Differential Similarity
F 3rd order polynomial
G 4th order polynomial

Empirical Testing (including cross validation)

Conclusions

Residuals after fit

→ 4th order polynomial

Prediction (external test)

→ Any model except 4th order polynomial

Not enough of a difference between models to justify statistical parameter significance testing

→ use lowest order model

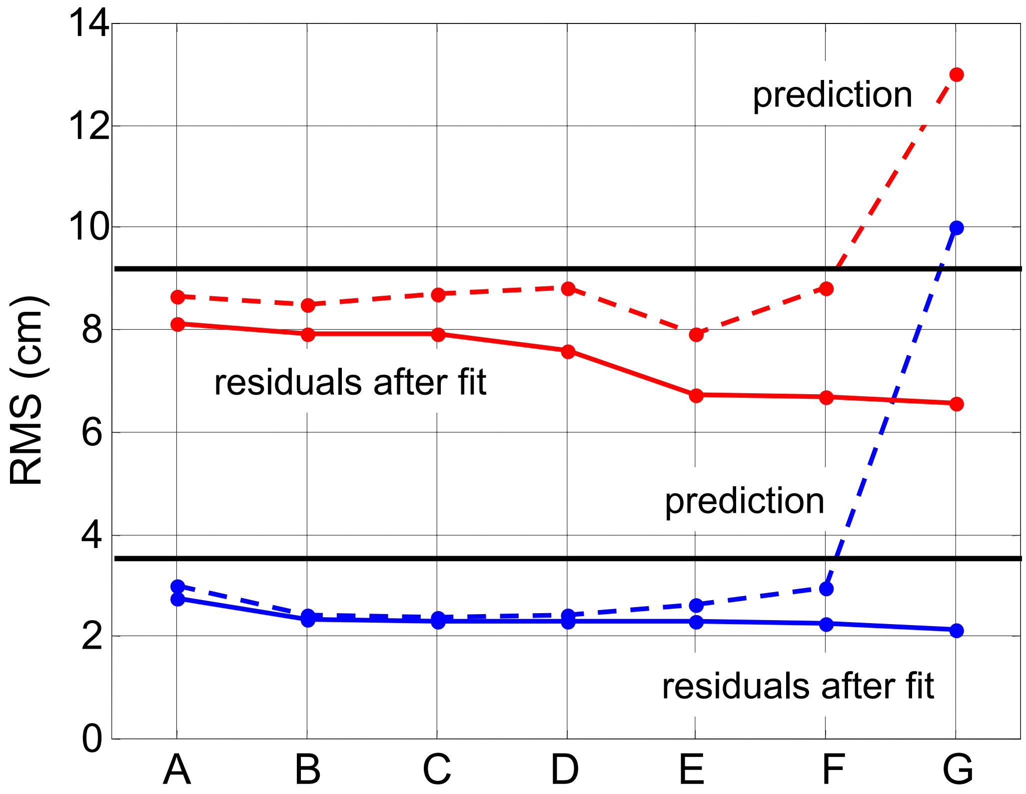

Switzerland Canada

Results - Switzerland

Classic 4-parameter fit

$$1 \quad \cos\varphi\cos\lambda \quad \cos\varphi\sin\lambda \quad \sin\varphi$$

Selection criteria

R^2	0.5668
$\overline{R}^2$	0.5181
$\sqrt{\hat{v}^T\hat{v}}$	24.5 cm
condition number	2.77×10^7
rms after fit	2.4 cm
rms (prediction)	2.4 cm

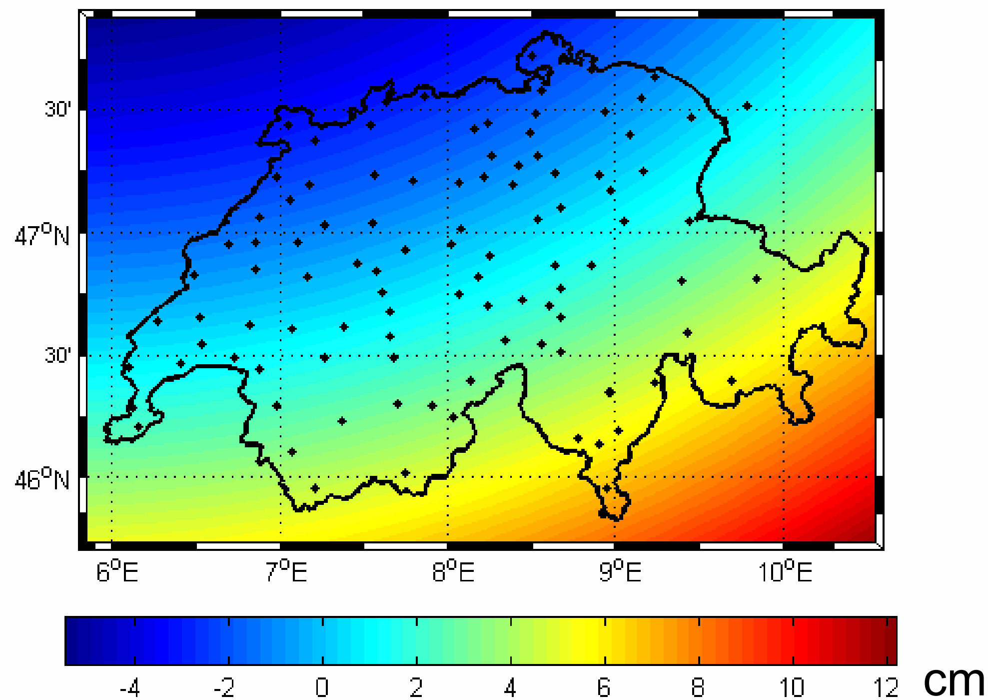

Results - Canada

Differential Similarity Fit (7-parameters)

$$\cos\varphi\cos\lambda \quad \cos\varphi\sin\lambda \quad \sin\varphi \quad \frac{\sin\varphi\cos\varphi\sin\lambda}{W} \quad \frac{\sin\varphi\cos\varphi\cos\lambda}{W} \quad \frac{1-f^2\sin^2\varphi}{W} \quad \frac{\sin^2\varphi}{W}$$

Selection criteria

R^2	0.4805
$\bar{R}^2$	0.2311
$\sqrt{\hat{v}^T\hat{v}}$	53 cm
condition number	1.52×10^{12}
rms after fit	6.7 cm
rms (prediction)	7.9 cm

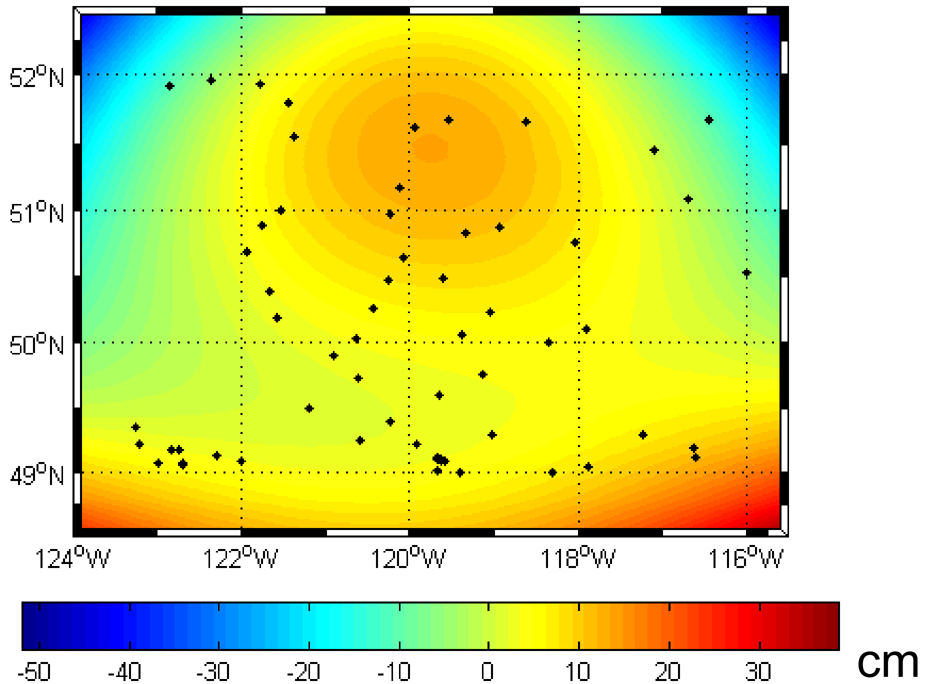

Summary

- **Semi-automated procedure** for **comparing parametric surface models** and **assessing model performance** was presented
- ***Semi***
  - no unique straightforward solution
  - some user intervention required
- In most cases, the best test is cross-validation (prediction)
  - independent 'external' test
  - depends on quality of data
- When model parameters are highly correlated (as is the case with polynomial regression), statistical testing may not be conclusive
- Use orthogonal polynomials to eliminate problems with high correlation between parameters (i.e. Fourier Series)
- Procedure should include a **combination** of empirical **<u>and</u>** statistical testing